IN VITRO LONG NONCODING RNA RESPONSIVENESS TO ISCHEMIC CONDITIONS IN FETAL SHEEP ISLETS

By

Ayna Tracy

____

A Thesis Submitted to the Faculty of the

DEPARTMENT OF ANIMAL AND COMPARATIVE BIOMEDICAL SCIENCES

In Partial Fulfillment of the Requirements

For the Degree of

MASTER OF SCIENCE

In the Graduate College

THE UNIVERSITY OF ARIZONA

2024

THE UNIVERSITY OF ARIZONA
GRADUATE COLLEGE

As members of the Master's Committee, we certify that we have read the thesis prepared by: Ayna Tracy

titled: In Vitro Long Noncoding RNA Responsiveness to Ischemic Conditions in Fetal Sheep Islets

and recommend that it be accepted as fulfilling the thesis requirement for the Master's Degree.

Sean W Limesand PhD (Aug 14, 2024 14:13 PDT)
Sean W Limesand PhD — Date: Aug 14, 2024

Ravi Goyal — Date: Aug 14, 2024

Chi Zhou (Aug 14, 2024 15:42 PDT)
Chi Zhou — Date: Aug 14, 2024

Final approval and acceptance of this thesis is contingent upon the candidate's submission of the final copies of the thesis to the Graduate College.

I hereby certify that I have read this thesis prepared under my direction and recommend that it be accepted as fulfilling the Master's requirement.

Sean W Limesand PhD (Aug 14, 2024 14:13 PDT)
Sean W Limesand PhD — Date: Aug 14, 2024
Thesis Committee Chair
ACBS

Acknowledgements

I would like to express my gratitude to everyone that has supported me throughout my journey as an Indigenous graduate student. Many programs and scholarships have supported me through these two years. I am grateful to the Alfred P. Sloan Foundation's Indigenous Graduate Partnership (SIGP) Program, the Office of Navajo Nation Scholarship & Financial Assistance (ONNSFA), W.T. and Winifred McClelland Scholarship (ACBS), and the Harry W. and Elsie M. Porterfield Scholarship for financially supporting me to earn my Master's in Animal and Comparative Biomedical Sciences.

Secondly, I would like to thank the Limesand lab members for the support and friendship that has been built over the last two years. I would like to thank Miranda Anderson for the encouragement and guidance through endless hiccups with cell culture and lab work. Thank you to Mariangel Valera, Sanya Kathuria, Daniel Chrisenberry, and Rosa Luna for the unwavering support that has gone beyond professional work. Working alongside you has been an incredible experience.

I would like to extend my thanks to the committee members for their feedback, guidance, and encouragement. Dr. Sean Limesand for guiding me through this research project and endless advice and teachings. Dr. Chi Zhou for supporting and teaching me since before my graduate career started when I was a post-baccalaureate. Dr. Ravi Goyal for advice, teachings, and encouragement when I was a TA.

Lastly, I have my heartfelt thanks to my friends and family members for their love and support that has been there every step of the way.

Land Acknowledgement

We respectfully acknowledge the University of Arizona is on the land and territories of Indigenous peoples. Today, Arizona is home to 22 federally recognized tribes, with Tucson being home to the O'odham and the Yaqui. Committed to diversity and inclusion, the University strives to build sustainable relationships with sovereign Native Nations and Indigenous communities through education offerings, partnerships, and community service.

Table of Contents

List of Figures and Tables

Abstract

Fetal growth restriction (FGR) predisposes offspring to long-term health risks, such as Type 2 Diabetes and obesity. They have a higher risk of developing glucose intolerance due to impaired insulin secretion. Placental insufficiency causes fetal hypoxemia and hypoglycemia in FGR fetus leading to β-cell dysfunction from reduced β-cell mass. Long noncoding RNAs (lncRNA) are regulatory molecules that modulate transcriptional and post-transcriptional processes, and high-throughput RNA sequencing data identified several differentially expressed lncRNA in FGR islets versus controls. The objective of this study was to determine ischemic responsiveness of these differentially expressed FGR lncRNAs in control islets in vitro and develop an in vitro hypoxic/ischemic cell line model that shows responsive MALAT1 expression and NF-kB activity. The islets were isolated from fetal sheep and were cultured in ischemic and optimal conditions. MIN6 and INS832 cells were cultured in hypoxic conditions (200-250 uL/mol $CoCl_2$ or 1% O_2) for 24 hours. Western blot was conducted to measure p50 and p65 subunit translocation and luciferase assay was conducted to measure NF-κB response. oFUVECs were cultured in 1% O_2 for 24 hours. We found that in vitro islet ischemia significantly altered for six of the nine lncRNAs. Among these, MALAT1 and H19 concentrations were higher ($P<0.05$), and SI-linc20-39a, LINC28868, SI-linc9-103, and RUNX1T1 Carmen concentrations were lower ($P<0.05$). Hypoxic oFUVECs only showed 7-fold high expression in H19 and no changes the remaining lncRNAs. MALAT1 and NF-kB expressions did not change in response to hypoxic (1% O_2) in insulinoma cells lines. NF-kB activity increased with $CoCl_2$-treated MIN6 cells. We found no alternative splicing for MALAT1 transcript and confirmed the coding potential for five lncRNAs. Our data confirmed the MALAT1 as a lncRNA with minimal coding potential with no detection of alternative splicing. Because we could not find a working insulinoma cell that shows responsive MALAT1 and NF-kB, primary fetal sheep islets may be the ideal in vitro model to investigate the regulatory roles of MALAT1 in FGR islets.

Chapter 1

Fetuses born with fetal growth restriction are at higher risk of neonatal and perinatal morbidity and mortality (Kaijser et al., 2009). On a global scale, 10% of all pregnancies, which is 10 million babies every year, are affected by fetal growth restriction (FGR) (Colella et al., 2018). Prevalence of FGR is greater in under-developed countries by more than six times compared to developed countries. In the United States, approximately 5% of pregnancies are affected by FGR and these infants have a higher risk of developing metabolic diseases later in life, including diabetes mellitus and obesity (Kaijser et al., 2009). FGR is defined as a fetus that is unable to grow to its full genetic potential due to multiple underlying causes (Nardozza et al., 2017; Kamphof et al., 2022).

Placental insufficiency is the leading cause of FGR compared to maternal, genetic, and fetal factors. Clinical diseases, chromosomal abnormalities, and infections are potential maternal and fetal factors that can also cause FGR, although the etiology of placental insufficiency is usually unknown (Nardozza et al., 2017). Fetuses exhibit hypoxemia, hypoglycemia, acidosis, and have elevated norepinephrine concentrations as a consequence of growth restriction, and there are ongoing investigations on the mechanisms of fetal programming (Niet-Diaz et al., 1996, Nicolini et al., 1990, Okamura et al., 1990; Pardi et al. 1993). Currently, clinical interventions are limited to close observations because there are no treatments for babies diagnosed with FGR (Kamphof et al., 2022).

Characteristics of FGR in humans

Diagnosing FGR begins with screening the growth of the fetus. FGR fetuses are typically born with low birth weight classifying them as small for gestational age (SGA). SGA is defined as a birth weight below the 10^{th} percentile of the population for that given gestational age. However, fetuses that are constitutionally small are not always classified as FGR. Hence, SGA is not a consequence of genetic or health related growth reduction (Osuchukwu & Reed, 2020). In clinical settings, the abdominal circumference (AC) and head circumference (HC) are measured to estimate fetal weight during pregnancy using ultrasound (Kamphof et al., 2022). Late onset FGR occurs during the 3^{rd} trimester of pregnancy when the fetus is rapidly growing. Strikingly, when the growth falters due to insufficient nutrients and oxygen this can lead to asymmetrical FGR where the fetal head to abdominal circumference ratio is disproportioned (Nardozza et al., 2017). Low AC is indicative of thinness and smaller liver size and muscle mass (Nardozza et al., 2017; Chew & Verma, 2020). FGR fetuses, therefore, are diagnosed with higher biparietal diameter to abdominal circumference ratio making them asymmetrical FGR (Barry et al., 2008).

FGR is predicted through Doppler ultrasound velocimetry assessment during pregnancy to detect vascular resistance (Nardozza et al., 2017; Pardi et al., 1993). During an uncomplicated pregnancy, uterine blood flow increases 2.5-folds during the second half of pregnancy to meet the needs of the growing fetus (Reynolds et al., 2006; Thornberg & Louey, 2013). The umbilical blood flow increases proportionally with fetal weight up to 20 weeks before declining (Acharya et al., 2006). Therefore, disruption to normal rates of uterine and umbilical blood flows are crucial components for FGR diagnosis. Absent or reverse end diastolic flow in umbilical arteries are indicative of placental vascular resistance and are associated with FGR. Reduced uteroplacental perfusion lowers nutrients and oxygen uptake due in part to abnormal placentation (Nardozza et al., 2017). Abnormal placentation ultimately leads to placental dysfunction and asymmetrical FGR. In addition to AC:HC ratios, asymmetric growth is also determined by the middle cerebral artery blood flow (relative to placental blood flow resistance) measurement that shows hemodynamic distribution within the fetus to determine the possibility of brain sparing, which redistributes blood to vital organs at the expense non-vital organs such as the skeletal muscles and kidneys (Kamphof et al., 2022). Hence, PI-FGR fetuses show higher umbilical artery doppler pulsatility index and lower uterine and umbilical blood flows (Barry et al., 2008, Rigano et al., 2001).

Aside from low birth weight and hemodynamic abnormalities, the pathophysiology of placental insufficiency induced FGR also includes impaired insulin secretion and glucose metabolism (Colella et al., 2018; Barry et al., 2008). The pancreas is composed of acinar cells and islet of Langerhans, which are composed of β-cells that secrete insulin, α-cells that secrete glucagon, δ-cells that secrete somatostatin, and PP cells that secrete pancreatic polypeptides. Insulin, an anabolic hormone, regulates glucose homeostasis and is important for fetal growth (Fowden A., 1992). Disrupting insulin production and secretion has been proven to cause fetal growth restriction by reduction of glucose uptake, utilization, and oxidation (Fowden A., 1992). Newborns diagnosed with growth restriction exhibited hypoinsulinemia and hypoglycemia (Niet-Diaz et al., 1996, Nicolini et al., 1990). The islets of Langerhans were small in growth restricted infants compared to infants born from normal pregnancies. Specifically, they have a significantly lower percentage of β-cell population (Van Assche et al., 1977). Children born SGA showed catch-up growth by 1 year of age had developed lower insulinogenic index and lower glucose-stimulated insulin secretion (GSIS) at age 4 (Milovanovic et al., 2014). After childhood, adults that were born with FGR exhibited glucose intolerance and mild diabetes (Phipps et al., 1993). In addition, young men that were born with low birthweight exhibited impaired glucose tolerance and low insulin secretion by 30% (Jensen et al., 2002). These data from these epidemiological studies suggest that the pancreatic β-cell function in humans continues to decline over time in conjunction with glucose intolerance after an initial bout with growth restriction during pregnancy.

In summary, the fetal signs of FGR are caused by insufficient oxygen and nutrient transport across the placenta that lowers placental mass, altered placental morphology, and reduced oxygen and nutrient transport capacity (Regnault et al., 2002; Nieto-Diaz et al., 1996). Downstream effects in the fetus are hypoglycemia and hypoxemia that disrupt endocrine pancreas formation and function, which does not fully return to normal. Human studies found that infants born with FGR exhibited reduced insulin secretion (Van Assche et al., 1997). Studies have also associated impaired insulin secretion manifested in childhood and adulthood with low birth weight (Jensen et al., 2002; Milovanovic et al., 2014). This leads to the onset of glucose intolerance, insulin resistance, and loss of normal glucose homeostasis (Béringue et al., 2002, Jensen et al., 2002). These factors increase the risk of developing long-term health consequences like coronary heart disease, diabetes mellitus, obesity, and hypertension. Established FGR animal models have investigated underlying mechanisms of FGR in perinatal and post-natal events that link pancreatic dysfunction and impaired peripheral insulin signaling with metabolic disorders.

FGR Animal Models

In addition to epidemiological studies, human FGR has been investigated in-depth by *ex vivo* and *in vitro* techniques with placental tissue and cellular research (Rigano et al., 2001; Nieto-Diaz et al., 1996, Béringue et al., 2002). However, limitations for studying human pregnancies narrow the scope of *in vivo* research on FGR. Several animal models of FGR exhibit FGR characteristics reminiscent of those in human fetuses and are used to investigate the underlying mechanisms and consequences of FGR. Even with partial overlapping similarities in reproductive physiology, FGR models have been developed in ruminant and rodents to mimic the pathophysiology seen in human. Animal FGR models provide a broader representation of FGR that covers the maternal, placental, and fetal aspects (Barry et al., 2008). Multiple variables are considered when choosing models based on the advantages and disadvantages regarding the purpose of the study, such as gestational length, fetal number, and fetal-maternal interface of the species (Swanson & David, 2015). Fetal and maternal interventions to mimic growth restriction have been established to investigate pancreatic dysfunction (Frantz et al., 2011; Simmons et al., 2001; Limesand et al., 2005; Limesand & Hay, 2003).

Rodent model

Several FGR rodent models have had a significant impact on developmental programming investigations helping to elucidate pancreatic dysfunction in offspring. Maternal dietary restriction with a low-protein diet (LP) had rat pups with fewer islet numbers and altered islet cell type distribution. Strikingly these results prevail in low-birth-weight offspring only in F1 generation, but pancreatic mass and islet diameter were significantly lower compared to control pups across F1 to F3 generations (Frantz et al., 2011). The offspring of nutrient-restricted mice showed growth restriction in utero and glucose intolerance at 6 months demonstrating glucose intolerance reminiscent of human FGR populations (Radford & Han, 2019). Rats that were born from uterine artery ligated IUGR developed decreased β-cell function, glucose intolerance, and insulin resistance that later led to type 2 diabetes phenotype (Simmons et al., 2001). These rodent studies provide insights into post-natal, life-long, and transgenerational effects of FGR on the endocrine pancreas.

Neonatal rodents are also born underdeveloped and β-cell expansion and proliferation occurs at postnatal stages of life (Aguilera et al., 2022; Sanches-Parra et al., 2018). Islets in prenatal stages do not have a fully developed insulin secretion response to glucose but are responsive to amino acids, which can be challenging to test glucose-stimulated insulin secretion (Hellerström & Swenne, 1991; Bonner-Weir et al., 2016). In addition, rodents have a shorter gestation length with narrow windows for fetal therapies. Investigating physiological aspect is challenging due to the small size of the fetus. Rodent FGR research investigates FGR mostly by measuring placental to fetal weight ratio, pup survival, post-natal growth, and uterine and umbilical blood flow (Rueda-Clausen et al., 2014; Frantz et al., 2011; Radford & Han, 2019; Constância et al., 2002). Although life-course studies of FGR provide insight into long-term consequences of β-cell dysfunction, detecting the primary mechanisms is limited, whereas fetuses from larger animal models can be investigated more.

Sheep model

Sheep allow longitudinal investigations during gestation, which include in vivo and in vitro experiments in the fetus. Pregnant sheep have served as long-standing model for human pregnancy because they have singleton pregnancies with similar birth weights and gestational lengths that are longer than rodents (Swanson & David, 2015). Furthermore, fetal and maternal circulation can be sampled with the surgical placement of indwelling catheters (Meschia et al., 1969). Therefore, pregnant sheep have the advantage of using consecutive blood sampling from both mother and fetus through catheterization to investigate the fetal and placental physiology, metabolism, and endocrine status (Barry et al., 2008, Darby et al., 2020). Several models of FGR have been established in pregnant ewes, which provides additional opportunities to investigate the pathophysiology of pregnancy (Galan, et al., 1999; Regnault et al., 2003). These models of FGR are created by maternal hypoxia, hyperthermia, undernutrition, and overnutrition. Placental restriction-induced FGR can also be induced by surgically manipulation through placental embolization and maternal caruncIectomy (Swanson & David, 2015; Regnault, 2003). The naturally occurring maternal hyperthermia model has been shown to induce placental insufficiency and FGR and is reliably used by several laboratories to study severe FGR (Regnault et al., 2002; Barry et al., 2008; Regnault, 2003).

In normal pregnancy, the villous membranes of the sheep placenta undergo rapid growth after 5 days of gestation and evidently form indentation of fetal capillaries in epithelial layer after 100 days (Stegeman, 1974). The developed epithelial layer separates fetal and maternal blood that is essential for exchanging metabolic substrates such as oxygen and glucose (Stegeman, 1974). Maternal hyperthermia-induced placental insufficiency is produced with warm ambient temperature during mid-gestation when placental growth is maximum (Bell et al., 1987; Bell et al., 1989; Limesand et al., 2005; Leos et al., 2010; Macko et al., 2013). The process of inducing placental insufficiency occurs by the ewe has to increase blood flow to the skin and lungs to dissipate heat, which decreases the blood flow of internal organs such as the uterus (Limesand et al., 2018). This leads to a decrease in uterine and umbilical blood flow and reduces placental growth and maturation. In a study on heat-stressed ewes, it was hypothesized that the epithelial layer at the maternal-fetal interface did not correctly grow and differentiate (Regnault et al., 2007). So, heat stress leads to smaller placenta with lower permeability for glucose and oxygen (Regnault et al., 2007; Thureen et al., 1992). This effect lowers the placental transport capacity for glucose and oxygen, produces fetal hypoglycemia and hypoxemia, and contributes to its decline in fetal growth and metabolism (Regnault, 2003; Limesand et al., 2018).

The maternal hyperthermia sheep model of placental insufficiency has physiological and biochemical effects on the fetus that replicate those seen in human fetuses with FGR. In the sheep model, umbilical and uterine artery blood flows are reduced in growth-restricted groups compared to thermoneutral controls (Bell et al., 1989; Thureen et al., 1992). By 0.9 gestation, fetal weights were lighter compared to control fetuses whereas placental weights were ~40% lower at 0.7 gestation and remained lighter through the final third of gestation (Thureen et al., 1992; Limesand et al., 2013; Macko et al., 2013). Most visceral organs and peripheral tissues are reduced to a similar extent as fetal weight in the FGR fetus. However, brain-to-liver ratio is increased, which reflects brain sparing. Alternatively, the endocrine mass of the pancreas was reduced to a greater extent than pancreas weight, which establishes targeted reductions of β-cell mass (Limesand et al., 2005; Limesand et al., 2013). These variations in fetal weight and relative tissue ratios are fetal adaptations to hypoglycemia, hypoxemia, hypoinsulinemia, and hypercatecholaminemia (Limesand et al., 2005; Leos et al., 2010; Limesand et al., 2013). Near term, plasma glucose concentrations are ~50% lower in PI fetal sheep compared to controls

(Limesand et al., 2007). Arterial blood partial pressure of oxygen and oxygen contents were reduced >30% (Leos et al., 2007; Limesand et al.,2007; Limesand et al., 2013). Catecholamine concentrations, such as norepinephrine, were increased by 3-folds in PI fetuses at 0.7 gestation and increase by 4-fold by near term (Limesand et al., 2006; Macko et al., 2013). Altogether elevated norepinephrine concentrations and low glucose and oxygen concentrations have been shown to cause β-cell dysfunction in FGR fetus by lowering insulin secretion, insulin content, and β-cell mass (Limesand et al., 2006; Macko et al., 2013). Thus, maternal hyperthermia-induced placental insufficiency in pregnant sheep is the ideal model to investigate the underlying mechanisms of FGR β-cell dysfunction.

Impaired Insulin Secretion

The endocrine cells of the fetal pancreas is essential for fetal growth and metabolism in utero and post-natally (Fowden et al., 1989; Jabary et al., 2023; Hay et al., 1988). Specifically, insulin and glucagon regulate glucose concentrations in the blood by regulating gluconeogenesis in liver and glucose uptake in other tissues, such as skeletal muscle (Fowden & Hay, 1988). By the third trimester of gestation, β-cells in fetal islets secrete insulin in response to increasing blood glucose concentrations (Limesand et al., 2006). In addition, insulin promotes tissue growth in the fetus, indicating that it coordinates growth with nutrient supply (Fowden & Hay, 1988). FGR fetuses with low glucose and oxygen concentrations have impaired insulin secretion due to β-cell dysfunction that contributes to lower fetal growth rate (Limesand et al., 2006)

Multiple factors underlie the β-cell impairments in PI-FGR fetal sheep models (Green et al., 2010). Hypoxemia contributes to reduced insulin secretion by increasing catecholamine concentrations (Leos et al., 2010). Specifically, norepinephrine was shown to inhibit glucose stimulated insulin secretion (GSIS) in FGR fetuses by stimulating the α2-adrenergic receptor (Leos et al., 2010; Macko et al., 2013). Here the investigators infused adrenergic receptor antagonists to inhibit norepinephrine stimulation of the α-adrenergic receptors and measured glucose-stimulated insulin concentrations in control and FGR fetuses using a square wave hyperglycemic clamp technique. They found that FGR fetal GSIS responsiveness during the adrenergic blockage was 7.1-fold higher during hyperglycemia and 4.1-fold higher during euglycemia, which indicated that adrenergic stimulation of α2-recptors inhibited insulin secretion (Leos et al., 2010; Macko et al., 2013). Strikingly when norepinephrine was infused chronically for 7 day in normal sheep fetuses insulin secretion increased following sensation of the NE infusion, indicating that chronic adrenergic stimulation can cause β-cell adaptations. These findings were supported in human studies that showed higher NE and metabolite concentrations in FGR fetuses lead to higher insulin concentrations in infants (Greenough et al., 1990).

Along with impaired insulin secretion, insulin sensitivity was enhanced in fetuses in the FGR sheep model (Limesand et al., 2007). The fetal glucose-to-plasma insulin ratio (G/I) was greater in late gestation (Limesand et al., 2013). Furthermore, radiolabeled glucose tracer studies showed net rates of fetal glucose utilization were not different between control and FGR fetuses, but insulin concentration were significantly lower, which supports greater insulin sensitivity (Brown et al., 2024). Glycogen content was 2.2-fold higher in skeletal muscle of IUGR compared to controls, but lower hepatic glycogen content (Limesand et al., 2007; Brown et al., 2024). Altogether, greater insulin sensitivity in FGR fetuses promotes glucose utilization in peripheral tissues, but because of the rate of placental glucose uptake is reduced the near normal glucose utilization rate in FGR fetuses depends on hepatic glucose production (Limesand et al., 2007, Thorn et al., 2009).

Islets and β-cells in Fetal Pancreas

Aside from impaired insulin secretion and greater insulin sensitivity, the origin hypoinsulinemia begins in the islets of the pancreas. A hyperthermia-induced placenta insufficiency sheep study reported significant reduction in endocrine pancreatic mass relative to the fetal mass of FGR (Limesand et al., 2005). In vivo islet response showed growth-restricted fetuses exhibiting impaired GSIS by presenting 64% lower insulin concentrations at basal glucose concentrations and 76% lower at hyperglycemic clamp in comparison to normal fetuses (Limesand et al., 2006).

In-vitro islet response to low and high glucose concentrations showed that insulin secretion from β-cells was impaired in FGR fetuses. Islets isolated from control and FGR fetuses were incubated in 1mM (low) glucose, 11.1mM (high) glucose, and 30 mM KCl concentrations to measure insulin release. The secretion data was normalized to the islet number or insulin content, which was 82% lower in FGR islets than control islets. Normalization to insulin content showed that there was higher fractional insulin release with 11.1mM glucose and 30 mM KCl incubations in FGR islets compared to controls (Limesand et al., 2006). This was because insulin content was lower in FGR islets. In contrast, the absolute amount of insulin secreted per FGR islet was lower in response to secretagogues. These findings indicated that insulin synthesis and storage were disrupted. Oxidative glucose metabolism was also lower in FGR islets, which indicates that oxidative phosphorylation was impaired by FGR (Limesand et al., 2006).

Histology data showed that the number of β-cells was reduced and they have lower β-cell mass. FGR fetuses had lower insulin content and insulin expression, which is partially explained by lower β cell mass (Limesand et al., 2005). Immunohistochemistry results showed significant decreases β-cells with phosphorylated histone H3 in FGR fetuses compared to control indicating that β-cell mitosis rates were reduced. β-cell apoptosis was ruled out because no differences were detected in TUNNEL plus insulin between FGR and control pancreata. Other endocrine cells, such as such as α-, δ-, and PP- cell area did not differ. This study concluded that nutritional deficiency reduces β-cell number by slowing β-cell proliferation. (Limesand et al., 2006; Limesand et al., 2005).

Molecular regulation of fetal β-cell dysfunction

At the molecular level, insulin mRNA expression is lower in FGR fetuses compared to controls (Limesand et al., 2005). Insulin mRNA was 66% lower in FGR islets relative to β-actin mRNA whereas glucagon, somatostatin, and pancreatic polypeptide mRNA concentrations did not differ (Limesand et al., 2005). In addition, a transcription factor, Pdx1, mRNA expression was also lower (Limesand et al., 2005, unpublished). Pdx1 regulates insulin gene expression in response to glucose and glucagon and plays a role in β-cell development and maturation (Spaeth et al., 2017; Ahlgren et al., 1998; Stoffers et al., 1997). Together, decreased transcription factors and insulin expression may contribute to lower insulin synthesis. These findings indicate impaired β-cell function may have underlying transcriptional programming mechanisms.

To determine the fundamental processes of impaired pancreatic islet function in FGR fetuses, Kelly, et al. (2017) conducted high throughput RNA sequencing on pancreatic islets from control and FGR fetuses. They identified 679 annotated genes to be downregulated and 386 upregulated annotated genes in FGR. Functional analysis on these differentially expressed genes identified enrichment in immune, metabolic and cellular structure-related pathways specifically gene were related to glucose metabolism, exocytosis, and cell cycle regulation. CDK19 and CDKL5 genes were higher in FGR islets suggesting that replication was reduced (Kelly et al., 2017). The RNA sequencing analysis followed up with downregulated proapoptotic Bax gene and no significant changes in other Bcl2 apoptotic proteins (Kelly et a., 2017). Therefore, the transcriptional analysis complement histological data previously discussed that showed reduced β-cell mitosis rate (Limesand et al., 2005).

The islet transcriptomic data has also found common molecular components that control β-cell survival, development, and proliferation. Nerve Growth Factor (NGF) was downregulated in FGR islets (Kelly et al., 2017). One study investigated NGF by conducting NGF withdrawal in human β-cells and found that NGF was antiapoptotic demonstrating NGF regulates β-cell survival (Pierucci et al., 2001). Another study showed NGF and one of its receptors, called Tak-A, were expressed during early development in rat pancreatic tissue. Furthermore, Tak-A was expressed at different points of cell differentiation in embryonic stages (Miralles et al., 1998). Regarding proliferation, the RNA-seq analysis has also found genes related to cell cycle arrest and proliferation such as TGF-β and REG3A, that were downregulated. TGF-β is involved in β-cell differentiation and development in embryonic islets and β-cell function in adult islets of mice (Smart et al., 2006; Harmon et al., 2004). These common molecular components may play pivotal roles in cell development, differentiation, and maturation in fetal islets.

RNA sequencing analysis found differentially expressed hypoxia responsive genes in growth restricted islets (Kelly et al., 2017). Hypoxia-inducible factor 3α (HIF3α) subunit and vascular endothelial growth factor receptor (VEGFR) genes were upregulated in growth restricted fetuses. HIF1α is generally post-translationally regulated by hypoxia with no change in mRNA expression levels, but HIF3α mRNA expression increased. This process reflects the in-utero hypoxemia state of the fetus, which exhibits low oxygen content (Limesand et al., 2013). These hypoxic-induced responses in fetal islets raise the question for adaptative responses these islets undergo in hypoxemic environment (Kelly et al., 2017). Islet function is dependent on islet vascularization for oxygen, nutrients, and hormone paracrine signaling. Hormones, like VEGF and HGF, expressed in β-cells and endothelial cells play a role in islet vascularity and insulin secretion (Rozance et al., 2015). Studies have shown that growth restricted fetuses display impaired vascularity and hormone production in the pancreas.

Summary

FGR fetuses are predisposed to long term health consequences such as diabetes mellitus. Impaired GSIS, lower β-cell mass, and smaller islet size are hallmarks of pancreatic dysfunction in FGR fetuses. These differentially expressed genes demonstrate underlying molecular mechanisms that are programming β-cell dysfunction in growth-restricted fetal islets. The transcriptomic analysis study, however, did not evaluate the differentially expressed long non-coding RNAs. The lack of functional analysis on lncRNAs in β-cell dysfunction of growth restricted islets is due to lack of annotated genes in the sheep genome. The purpose of this study is to determine and analyze differentially expressed lncRNAs found in the RNA sequencing analysis that have potential roles in islet dysfunction in growth restricted fetuses.

Chapter 2

Functional Roles of Long Noncoding RNAs

In the RNA sequencing data by Kelly et al., (2017), long noncoding RNAs (lncRNAs) were also differentially expressed in growth-restricted islets but were not further evaluated. Amongst several classes of RNA, lncRNAs are non-protein coding RNAs greater than 200 nucleotides with short open reading frames (ORFs). LncRNAs can be classified as long intergenic noncoding RNAs (lincRNAs), intronic noncoding RNAs, antisense RNAs, and nonsense noncoding RNAs (Kumar & Goyal, 2017). Recent studies revealed novel functions of lncRNAs to be involved in biological processes, such as chromatin modification, transcriptional regulation, translational regulation, and post-translational regulation by interacting with mRNA, DNA, miRNA, and proteins (Zhang et al., 2019; Statello et al., 2020; Schmitz et al., 2016). Over 1100 lincRNA and antisense lncRNAs were identified in human islet transcriptome and 47% were orthologous to mouse transcripts (Morán et al., 2012). Of the 1100 lncRNAs identified, 55% lincRNA and 43% of antisense lncRNA were transcribed as islet-specific lncRNAs (Morán et al., 2012). Studies showed abundant lncRNA expression across various diseases, such as cancer, cardiovascular diseases, and diabetes mellitus (Statello et al., 2020; Zhang et al., 2019). Particularly, studies that focused on Type 2 Diabetes (T2D) have identified regulatory roles of lncRNAs in human pancreatic β-cells (Akerman et al., 2017).

LncRNAs have been shown to modulate β-cell transcriptional activity and have functional roles in insulin release. A study conducted loss of function experiments to measure transcriptional responses by knocking down different lncRNAs in human β-cell lines. LncRNA knockdowns resulted in transcriptional changes in nearby genes indicating cis-regulatory processes. In addition, HI-LNC12, HI-LNC78, and HI-LNC71 knockdown led to lower GSIS in EndoC-βH3 cells (Akerman et al., 2017). Another study showed significantly lower expression of β long intergenic long noncoding RNA 3 (βlinc3) in mice and humans exhibiting T2D. Further experiments showed βlinc2 overexpression and downregulated βlinc3 leading to higher apoptosis in MIN6 and mouse islets, although it did not affect the insulin expression, content, or secretion (Motterle et al., 2017). An in vivo study generated βlinc1 knockout mice that exhibited insulin resistance and lower GSIS. They found that βlinc1 knockout mice had 50% lower β-cell population in the pancreas compared to normal mice (Arnes et al., 2016). Genes related to β-cell maturation and development were also dysregulated in pancreas from βlinc1 knockout mice (Arnes et al., 2016). These studies demonstrate the transcriptional regulatory roles of lncRNAs on insulin secretion and islet development.

Interactions between LncRNAs and Transcription Factors

Islet function is an integral part of T2D pathogenesis and studies have identified regulatory roles of lncRNA interactions with β-cell-associated transcription factors (TFs) (Akerman et al., 2017; Morán et al., 2012). Transcription factors such as Pdx-1 and NeuroD, are essential for β-cell differentiation and insulin expression in response to changes of glucose concentrations (Melloul, 2004). To begin to define the lncRNA actions in islets, one study knocked down HI-LNC25 expression with shRNA and measured the mRNA expression of 24 genes responsible for regulating β-cell activity. They found that GLIS3 transcription factor, which is known to be highly expressed in β-cells of developing pancreas in mice, is positively regulated by HI-LINC25 (Morán et al., 2012; Senée et al., 2006). Another study conducted RNA-seq analysis and found PLUTO lncRNA to be downregulated in islets from patients with T2D and glucose intolerance (Akerman et al., 2017). Along with PLUTO, which is upstream from the Pdx-1 gene, Pdx-1 expression was also downregulated. Across multiple cells lines and primary islets, they confirmed that PLUTO regulated Pdx-1 because when PLUTO was knocked down using CRISPRi and gRNAs, the Pdx1 mRNA expression decreased. Furthermore, they found that PLUTO interacts with the chromatin to regulate the 3D chromatin structure and enhances transcription factor interactions between Pdx-1 promoter and upstream enhancer clusters. Therefore, PLUTO is regulating Pdx-1 activity in islets, but it's not the only lncRNA to regulate Pdx-1 (Akerman et al., 2017).

Another study investigated in vitro and in vivo reduction in insulin secretion by Meg3 lncRNA. Meg3 is predominantly expressed in pancreatic islets and was shown to be downregulated in diabetic mice (You et al., 2016). Further experiments demonstrated Meg3 suppression in mice and MIN6 cells led to impaired insulin secretion in response to glucose and increased β-cell apoptosis. To determine the cause of impaired insulin secretion, multiple transcription factors that were previously shown to be associated with β-cell function and maturation were measured by qPCR. They found that Pdx-1 and MafA expressions were lower with suppressed Meg3. This downstream leads to reduced insulin transcription and, in turn, decreases insulin protein synthesis (You et al., 2016). A similar study was conducted that downregulated TUG1 lncRNA and resulted in impaired GSIS as well as reduced Pdx-1, NeuroD1, and MafA TF expressions (Yinn et al., 2015). These studies demonstrate that lncRNAs regulate target gene expression by suppressing transcription factors that downstream impede insulin secretion and impair β-cell function.

MALAT1 lncRNA responsive to hypoxia

Metastasis-associated lung adenocarcinoma 1 (MALAT1), also known as NEAT2, is characterized as a long noncoding RNA longer than >7 kb in the human and >6.7 kb in the mouse genome (Hutchinson et al., 2007; Bernard et al., 2010). This highly conserved lncRNA can be localized in cytoplasm and nucleus (Hutchinson et al., 2007). It is expressed in nearly all tissues with the highest expression in the pancreas and lung (69, 70). MALAT1 has been extensively studied in neural development (Bernard et al., 2010), skeletal myogenesis (Watts et al., 2013), and vascular growth (Michalik et al., 2014) and has pathological functions in cancer (Ji et al., 2003), cardiovascular, and neurological diseases (Zhang et al., 2017). MALAT1 has various molecular functions in transcriptional regulation, post-transcriptional regulation, and alternative splicing (Tripathi et al., 2010; Tano et al., 2010; Zhang et al., 2017). Dysregulation of MALAT1 has been shown to be responsive to oxidative stresses, such as hypoxia and inflammation, and is associated with pathological consequences.

MALAT1 is responsive to hypoxic and ischemic conditions in multiple cell lines and in vivo studies. In vitro studies demonstrated high MALAT1 expression in three different cancer cell lines in hypoxic environment of 0.2% O_2 and with HIF-1α knockdown (Lelli et al., 2015). In vivo studies show MALAT1 highly expressed in spleen, kidneys, testis, lung, and brain of hypoxic mice that were subjected to 8% O_2. Further investigations in spleen and testis showed hypoxia-induced MALAT1 expression in primary mouse kidney epithelial cells (Lelli et al., 2015). Another study showed renal ischemia/reperfusion in mice increased MALAT1 expression by 5-fold in kidneys compared to sham control groups (Tian et al., 2018). In the same study, in vitro $CoCl_2$-induced hypoxia increased MALAT1 expressions in HK2 cells by 3-folds. In addition, MALAT1 knockdown increased pro-inflammatory cytokines, IL-6 and TNF-α, that are associated with the NF-kB pathway (Tian et al., 2018). In vitro and in vivo studies demonstrated MALAT1 is not only oxygen-dependent, but it also has implications with inflammatory responses by interacting with NF-kB pathway in ischemic conditions.

Implications of MALAT1 on NF-kB Activity

Emerging evidence revealed mechanistic functions of MALAT1 regulating transcription factors. MALAT1 lncRNA has been associated as a negative regulator for Pdx-1 gene in islets of NOD mice islets and MIN6 cells (Ding et al., 2020). CHIP-Seq analysis showed decreased H3 histone acetylation of the Pdx-1 promoter in NOD mice and overexpression of MALAT1 decreased this acetylation, which suppressed Pdx-1 transcription and translation. NOD islet studies demonstrated enhanced insulin secretion when MALAT1 was suppressed and overexpressed Pdx-1 in response to high glucose levels (Ding et al., 2020). Another study has also found MALAT1 affects β-cell function in diabetic mice by regulating proteins and transcription factors that may be responsible for insulin biosynthesis (Xiong et al., 2020). These findings indicate that MALAT1 lncRNA is capable of influencing transcription factor activity and suppressing insulin secretion of β-cells.

Other transcription factors, such as NF-κB, has been shown to be essential for insulin secretion. NF-κB inhibition using Ipf1/IκBαM construct and PDTC, were treated in mouse islets and showed reduced insulin secretion in response to high and low glucose concentrations (Norlin et al., 2005). Niβ transgenic mice that had NF-κB inhibition exhibited mild diabetes with impaired glucose tolerance and GSIS in response to multiple islet secretagogues like arginine, carbachol, and glybenclamide. These secretagogues provide insight of insulin releasing mechanisms. They found slower rate of insulin release with arginine stimulation in Niβ mice compared to controls indicating disrupted insulin exocytosis. Niβ mice had decreased GLUT2 expression and insulin secretion in response to carbochol and glybenclamide indicating that glucose uptake and utilization were disrupted in islets of Niβ mice. This study demonstrated that physiological levels of NF-kB are essential for maintaining normal GSIS in β-cells in vivo and in vitro (Norlin et al., 2005).

NF-κB has been widely studied in various diseases and is known for its transcriptional activation of genes related to inflammation, cell proliferation, cell apoptosis, and cell differentiation (Oeckinghaus et al., 2011). Inflammatory-activated NF-κB has been shown to be regulated by MALAT1 lncRNA in human cell line macrophages (Zhao et al., 2016). Initially, LPS-induced inflammation upregulated MALAT1 and proinflammatory cytokines showed higher expression with MALAT1 knockdown after LPS stimulation. Furthermore, MALAT1 knockdown resulted in higher NF-kB activity with and without LPS stimulation. CHIP-Seq analysis showed MALAT1 knockdown increasing the binding of p65, a NF-κB subunit, on its target promoters demonstrating post-translational regulation. Lastly, they showed MALAT1 interaction with p50 and p65 subunits of NF-κB in the nucleus (Zhao et al., 2016).

Altogether, studies have demonstrated MALAT1 to be associated with β-cell function with regulatory transcription factor targets and is responsive to hypoxia and ischemia. Sheep fetuses with FGR fetuses have impaired GSIS, lower β-cell mass, and decreased insulin synthesis (Limesand et al., 2006). Moreover, deficiencies in insulin secretion persists in young lambs (Yates et al., 2019). To elucidate the mechanisms for pancreatic islet dysfunction, we have examined islet transcriptome in FGR fetuses using high throughout RNA-sequencing (Kelly et al., 2017). This transcriptomic analysis, however, did not evaluate the differentially expressed lincRNAs in FGR islets, which raises the question for potential underlying mechanisms of β-cell programming in growth-restricted fetal islets. Preliminary studies have already confirmed these differentially expressed lincRNAs in FGR islets by qPCR. MALAT1 expression is higher in growth-restricted islets by 3-folds (unpublished). In addition, RNA-sequencing analysis (Kelly et al., 2017) showed downregulated NF-κB target genes. Fetal sheep islets cultured in ischemic conditions showed 2-fold higher expression of MALAT1 compared to islets cultured in normal conditions. MALAT1 is well characterized in human and mouse genome, but still remains to be annotated in sheep islets. The objective of this study is to establish an in vitro hypoxia model using insulinoma cell lines that lower NF-κB activity and express MALAT1 mRNA. This research project aims to:

1. Sequence MALAT1 lncRNA transcript to determine potential alternative splicing in fetal sheep islets.
2. Determine whether the dysregulated lncRNA expressions found in the RNA sequencing study (Kelly, A., et al., 2017) are differentially expressed in ischemic conditions in fetal sheep islets.

3. Establish an in vitro cell model to test MALAT1 responsiveness and NF-kB activity in insulinoma cell lines.

Materials and Methods

Animals

All procedures involving animals the Guide for the *Care and Use of Laboratory Animals* and were approved by the Institutional Animal Care and Use Committee for the University of Arizona. Experimental groups and animal procedures for the FGR cohort has been published previously (Kelly et al., 2017). Six additional pregnant ewes with singleton control fetuses were used for islet isolations and in vitro islet experiments.

Islet Isolation

The postmortem dissections were performed at ~130 days gestational age (dGA). The fetal pancreas was infused with collagenase solution through the common bile duct then submerged in collagenase solution for digestion prior to islet isolation (Limesand et al., 2006). After separating islets from acinar cells, the islets were handpicked and cultured in RPMI 1640 media (GIBCO) containing 5% FBS (Hyclone, Cat # SH30088.03) and 2.8mM glucose. Islets were cultured in ischemic (<21% O_2, 0.5mM glucose) and optimal conditions (95% O_2, 2.8mM glucose) for 16 hours (n = 6).

Cell lines and Cultures

MIN6 and INS832 cell lines were cultured in 1640 RPMI media (GIBCO, Cat # 31800-022) containing 10% Fetal Bovine Serum (FBS) (Hyclone, Cat # SH30088.03) and 1X Penicillin Streptomycin (Sigma, Cat # P433). Primary ovine fetal umbilical vein endothelial cells (oFUVECs) (gifted by Dr. Chi Zhou, University of Arizona) were cultured and passed from P4 to P7 in Human

Endothelial Cell Medium (ECM) (Cell Biologics, Chicago, IL, Cat # H1168) with 5% FBS. oFUVEC purity was verified with GSI lectin and DAPI staining. All cells were cultured in humidified incubator at 37°C in 5% CO_2.

NF-kB Stimulation Treatment

NF-kB signal stimulator, TNF-α (R&D Systems, Minneapolis, MN, Cat # 10291-TA), was used to stimulate p50 and p65 translocation in MIN6 cells. After 24 hours hypoxia, the TNF-α treatment was administered at 20ng/ml for 20 minutes before lysing cells for western blot.

Hypoxia Treatment

Hypoxia treatment was administered by culturing in 1% O_2 or cobalt (II) chloride reagent ($CoCl_2$) (Sigma-Aldrich, St. Louis, MO, USA, Cat # 232696), which was dissolved in double distilled water. Prior to hypoxia treatment, cell media was pre-conditioned to hypoxia by incubated the media in sealed pressurized gas chambers (Billups-Rothenberg, Del Mar, CA, Pat # 5352414) overnight. oFUVECs, MIN6, INS832 cells were cultured in 1% O_2 in sealed pressurized gas chamber for 24 hours before RNA collection. MIN6 cells were cultured in 250 µmol/L $CoCl_2$ for 24 hours while INS832 cells were cultured in 200 µmol/L $CoCl_2$ for 24 hours prior to lysing cells for luciferase measurements.

Ischemic Treatments

A combination of low glucose concentration and $CoCl_2$ in 1640 RPMI media was administered to MIN6 and INS832 cell lines for 24 hours. There were no studies on $CoCl_2$ challenge on MIN6 and INS832 cell lines. Therefore, $CoCl_2$ concentrations were determined by culturing cells in various concentrations from 100 to 500 µmol/L and determined the best concentration based off the NF-kB response with luciferase and observations of cell death. For INS832 cells, 200 µmol/L $CoCl_2$ was determined to be the best concentration with optimal NF-kB response and no cell death observed. For MIN6 cells, 250 µmol/L $CoCl_2$ concentration was the optimal for NF-kB response and no observed cell death. Low glucose concentrations were 1mM glucose. Cells were treated with normal glucose levels at 11.1mM glucose.

5' RACE

To synthesize the 5' end of MALAT1 cDNA, the cDNA was amplified using the 5' RACE system (Thermo Fisher Scientific, Carlsbad, CA, Cat # 18374058). The first strand of cDNA was synthesized using reverse primer 5'-GCAAAGCAGTATCTCCGTATTCT -3'. The cDNA was purified using S.N.A.P. Column followed by TdT tailing and amplifying with PCR using Taq polymerase. The 5' RACE amplified product was then cloned and sequenced.

Cloning and Sequencing

MALAT1 primers were generated along predicted ovine MALAT1 sequence using sheep islet cDNA. MALAT1 products were amplified using Taq polymerase in CFX Connect Real Time PCR Detection System (Bio-Rad, Hercules, CA). The desired PCR products were confirmed in 1% agarose gel electrophoresis. PCR products were cloned in pCRII-TOPO vector linearized with 3'-thymidine overhangs (Thermo Fisher Scientific, Carlsbad, CA, Cat # 450640). Plasmids were transformed into electrocompetent One-Shot Mach1-T1 *E. coli* cells (Thermo Fisher Scientific, Carlsbad, CA, Cat # C862005). *E. coli* bacteria were plated in LB plates with 50ug/mL ampicillin and 40mg/mL X-Gal overnight. White positive colonies were picked and grown overnight in LB medium with 50ug/mL ampicillin. Plasmid DNA isolation was conducted by Wizard Plus SV Miniprep Purification System (Promega, Madison, WI, Cat # A1330). Cloned MALAT1 PCR products were confirmed by conducting EcoRI digest (Thermo Fisher Scientific, Cat # FD0274) followed by running 1% gel electrophoresis. DNA plasmids were submitted to the Arizona Genetics Core for Sanger Sequencing. Sequencing results were analyzed in Chromas and SnapGene viewer. After confirming efficiency of the sequencing results with T7 and Sp6 primers, the sequences were concatenated. CPC2 was used to analyze and determine the coding potential of the sequence and lncRNA identification.

Adenovirus transfection

The Ad-NFkB-Luc (Vector Biolabs, Malvern, PA, Cat # 1740) contains the Photinus pyralis (firefly) luciferase gene with five repeated NF-kB enhancer elements (TGGGGACTTTCCGC). Cells were transfected at 10-11 PFU/cell. Cells were incubated for 4 hours at 37°C before adding growth culture media. Cells were then incubated for 24 hours prior to starting hypoxia and ischemic treatments.

ONE-Glo Luciferase Assay

Cells were lysed with CelLytic MT cell lysis reagent (Sigma-Aldrich, St. Louis, MO, Cat # C3228) prior to adding ONE-Glo luciferase reagent. Lysis incubation time with luciferase reagent was 15 minutes at room temperature. Luciferase activity was measured in Clarity luminescence microplate reader (BioTeck, Winooski, VT). Parameter settings were Shaking: 1.00 Duration [s] Linear (Ampl.: 0.2mm, Freq.: 60min-1) / Delay: 1.00 Delay Time [s] / Measurement: 1.00

Measurement Time in [s]. Luciferase results were normalized with total protein by conducting BCA Reducing Agent Compatible (Thermo Fisher Scientific, Rockford, IL, Cat # 23252).

Lipofectamine 3000 transfection

MALAT1 knockdown with siRNA was conducted using lipofectamine 3000. One day after plating oFUVECs, the cells were transfected with siRNA using the Lipofectamine 3000 reagent according to the manufacturer's instructions (Thermo Fisher Scientific, Carlsbad, CA, Cat # L3000-008). The DNA-lipid complex was diluted in Opti-MEM medium (Thermo Fisher Scientific, Green Island, NY, Cat # 2491765). Prior to transfection, all wells were placed with ECM without antibiotics. Cells were incubated with DNA-lipid complex for 4 hours before replacing with ECM containing antibiotics and FBS. Cells were incubated for 48 hours prior to RLT lysis for RNA isolation.

MALAT1 siRNA

MALAT1 siRNA were designed from Integrated DNA Technologies DsiRNA Design Tool (Integrated DNA Technologies, https://www.idtdna.com/pages/products/functional-genomics/dsirnas-and-trifecta-rnai-kits). MALAT1 siRNA was dissolved in DEPC water and aliquoted to 10uM. oFUVECs siRNA treatment were divided into four experimental groups: untreated control, scrambled negative control, pooled MALAT1 siRNAs, siRNA 13.1, siRNA 13.5, and siRNA 13.6.

siRNA	**Strand**	**Nucleotide sequence**
Scramble Negative	Sense	5'-rCrUrUrCrCrUrCrUrCrUrUrUrCrUrCrUrCrCrCrUrUrGrUGA
	Antisense	rUrCrArCrArArGrGrGrArGrArGrArArArGrArGrArGrGrArArGrGrA
CD.Ri.476914.13.1	Sense	5'- rGrGrArCrUrUrUrGrArGrCrUrArArGrArUrGrArArUrGrUTT-3'
	Antisense	5'-rArArArCrArUrUrCrArUrCrUrUrArGrCrUrCrArArArGrUrCrCrArA-3'

CD.Ri.476914. 13.5	Sense	5’- rArUrArGrArArUrGrArArArArGrArArArGrCrUrArUrUrGGA-3’
	Antisense	5’- rUrCrCrArArUrArGrCrUrUrUrCrUrUrUrUrCrArUrUrCrUrArUrCrU-3’
CD.Ri.476914. 13.6	Sense	5’- rCrArArGrUrGrGrArArArUrGrUrUrArCrCrArArCrArGTT-3’
	Antisense	5’- rArArCrUrGrUrUrGrGrUrArArArCrArUrUrUrCrCrArCrUrUrGrCrC-3

Primer Design

MALAT1 transcripts were inputted in Primer3 design tool to generate primers along the transcript. Primer designs ranged from 400 to 700 bp. Sequence was confirmed after running in-silico PCR tool from UCSC Genome Browser before ordering.

Primers

Synthetic oligonucleotide primers were designed against the sheep genome sequence to verify islet specific expression. Lyophilized primers were dissolved to 10uM in TE Buffer. Uncharacterized sheep lncRNAs were generated based on chromosome number and base pair location on that chromosome.

Primers	Sequence 5’ to 3’	Species	GenBank	Anneal	Efficiency
LINC28868	F – CTCCACTAGGCTCTGCGTCT R – AGGTCTGAGCAGCAGAAAGC	Sheep	XM_027979478.1	62	92.7
SI-LINC 21-51 (LINC 28118)	F – TGATATGGTCCGGTGTGATG R – TCTTGAGGGTTCTGGGTGTC	Sheep	CP162293.1	61	100.1
SI-LINC 9-103 (LINC 28578 F2_R2)	F – ACTAGACAGACGGTGCCTGAA R – AAGTCCTGTCCTCTCCGTGTG	Sheep	CP162281.1	61	94.4
RUNX1T1_Carmen	F – AGCTCCAAATGCTGAGGTGT R – GACGACGAAGGGTTAATGGA	Sheep	CP162281.1	61	97.5
SI-LINC 7-41	F – CCAGCGTGTCAAAGAATCAA R – CTAGTGCCCAGTCGAGAAGG	Sheep	CP162281.1	60	102.2

SI-LINC 21-47 (MALAT1)	F – CGGGCGAGTGCTTAAGATAG R – TAGCGCCTACTCGTCAGGAT	Sheep	CP162293.1	60	90.1
SI-LINC 21-42 (LINC15) F2/R2	F – TGCAGGGTGGAGACAGGTTA R – CGGTGTCTGAGATCCGCTTG	Sheep	CP162285.1	60	97.2
LINC 20-39a	F – GCTTGCCTGGATTAGTCTGC R – CTCAAATCGCTGTCTCCACA	Sheep	CP162292.1	60	146.1
SI-LINC_X-27 F1/R1	F – CTCACCACAGACCCTGTTGAT R - TTTTGGCAGGCAGCTAGATAA	Sheep	CP162349.1	61	100.6
NFKB1	F – GACAGCACCACTTATGACGGA R – AGGAGTCATCCAGGTCGTACA	Sheep	XR_003589661.3	62	95.5
RELA	F – GCATCCAGACCAACAACAACC R – CAGCTCCCAGAGTTCCGATTT	Sheep	CP162293.1	62	95.7
LDHA	F – CATGGCCTGTGCCATCAGTA R – GGAAAAGGCTGCCATGTTGG	Sheep	CP162293.1	60	85.0
VEGFA	F – GGAGTACCCCGACGAGATAGA R – GGCTCACAGTGATTTTCTGGC	Mouse	NM_001025257.3	60	94.2
LDHA	F – TGGTCCAGCGAAACGTGAAC R – CGGTTTTTGGGAAAGCCACT	Mouse	XM_030242176.1	60	88.6
MALAT1	F – CACTTGTGGGGAGACCTTGT R – TGTGGCAAGAATCAAGCAAG	Mouse	NR_002847.3	60	87.1
MALAT1	F – CACTTGTGGGGAGACCTTGT R – TGTGGCAAGAGTCAAGCAAG	Rat	XR_010061180.1	60	99.8

RNA extraction and Real-Time PCR

Total RNA was extracted from cells using the Rneasy Mini Kit (Qiagen). First, cells were lysed using RLT buffer with 0.01% 2-Mercaptoethanol (Sigma M3148). Cells were shredded using the QIAshredder column (QIAGEN 79656). Using the RNeasy Mini Columns (Qiagen), RNA was washed with RW1 buffer then treated with DNase I (Qiagen) followed by repeated PW1 and RPE washes. RNA was eluted in 30ul RNase-free water. 1 ug of RNA was used to synthesize cDNA in triplicates using Reverse Transcriptase SuperScript III (Invitrogen 18080085). cDNA was diluted 1:2 or 1:3 and real time qPCR was conducted with SYBR Green Master Mix (Qiagen) in CFX Connect Real Time PCR Detection System (Bio-Rad). S15 housekeeping gene was used as internal normalization. The ΔCt was calculated and graphed for studies with less than 3 independent experiments. The $2\hat{} - \Delta\Delta Ct$ method was used to calculate the fold change of gene expression for studies with 3 or more independent experiments.

Nuclear protein extraction

MIN6 cells were treated in hypoxia (1% O2) for 24 hours in 100mm dishes. Three independent experiments were conducted with 2 replicates for each group. Cells were then challenged with TNF-α at 20ng.ml for 20 minutes. For nuclear extraction, cells were resuspended in ice-cold swelling buffer containing 10 mM Tris-HCl, 2 mM $MgCl_2$, and 3 mM $CaCl_2$. Cells were scraped out of the plate and repeatedly centrifuged and resuspended in swelling buffer +10% glycerol + 4U/ml Superase I mix and swelling buffer + 10% glycerol + 1% Igepal mix. Nuclei were washed with swelling buffer (containing 0.5% Igepal + 10% glycerol) followed by centrifugation (For

Igepal; Sigma-Aldrich, St. Louis, MO, Cat # I3021). The pellet was resuspended in lysis buffer containing protease inhibitors and stored in -80°C.

Western Blot

Prior to running gels, protein concentrations were measured using the BCA Reducing Agent Compatible according to the manufacturer's instructions (Thermo Fisher Scientific, Rockford, IL, Cat # 23252). MIN6 nuclear proteins were resolved in 10% gel at 60V for 30-45 minutes. The proteins were transferred to PVDF membrane and ran for 65 minutes at 100 V. Licor protocol (LI-COR) required transfer buffer containing 25mM Tris Base, 192 mM Glycine, and 20% methanol. The membrane was blocked with intercept blocking buffer provided by the LI-COR Revert 700 total protein stain kit (LI-COR, Lincoln, NE, Cat # D21122-01). Antibody for p50 and p65 were diluted in 0.2% Tween 20 to 1:1000 and incubated overnight at 4°C. The membrane was washed 4 times with 1X TBS-T containing 0.1% Tween 20. 1:15,000 Goat Anti-rabbit 800CW secondary antibody was incubated for 1 hour followed by 1X TBS-T and 1x TBS washes (LI-COR, Lincoln, NE, Cat # D11202-01). Membranes were scanned on Odyssey CLx Imaging System (LI-COR, Lincoln, NE). Results were analyzed on Empiria Studio Software.

Statistical Analysis

Data are presented as mean ± SEM of at least 3 independent experiments. Statistical significance was assessed by two-tailed T-test, mixed ANOVA, and one-way ANOVA.

Results

MALAT1 sequence and lncRNA protein coding potential

The sheep MALAT1 RNA nucleotide sequence (7299 bp) was determined from islet RNA to confirm the sequence homology and define alternative splicing. The sequencing results of 16 PCR clones were concatenated using NCBI BLAST alignment tools and SnapGene (Figure 1). The concatenated sequence aligned with the MALAT1 chromosomal DNA nucleotide sequence located in chr21:45469078-45476376 of Sheep genome, Oar_rambouillet_v1.02, for 7249 bp with 11 mismatches and 6 gap/insertions. The blue sequence represents the concatenated red sequences that were generated with PCR. To determine the coding potential of this transcript, the concatenated sequence was evaluated in CPC2. The Fickett score was 0.27943 with a complete putative ORF of 88 amino acids (Figure 2). The coding probability was 0.0871836, which classifies as a noncoding RNA sequence.

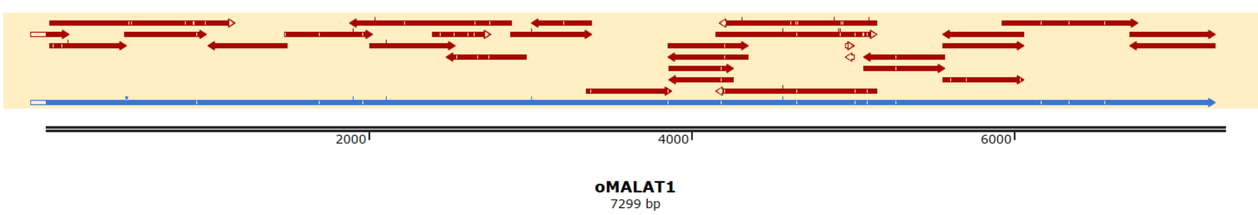

Figure 1. The MALAT1 sequence does not show evidence of alternative splicing. Forward and reverse primers were designed along the sheep MALAT1 chromosomal DNA sequence (black, chr21:45469078-45476376). These were amplified by PCR and cloned for sequencing, representing the red sequences. The blue sequence is the concatenated sequence that is aligned with the MALAT1 transcript in the double black line (7299 bp).

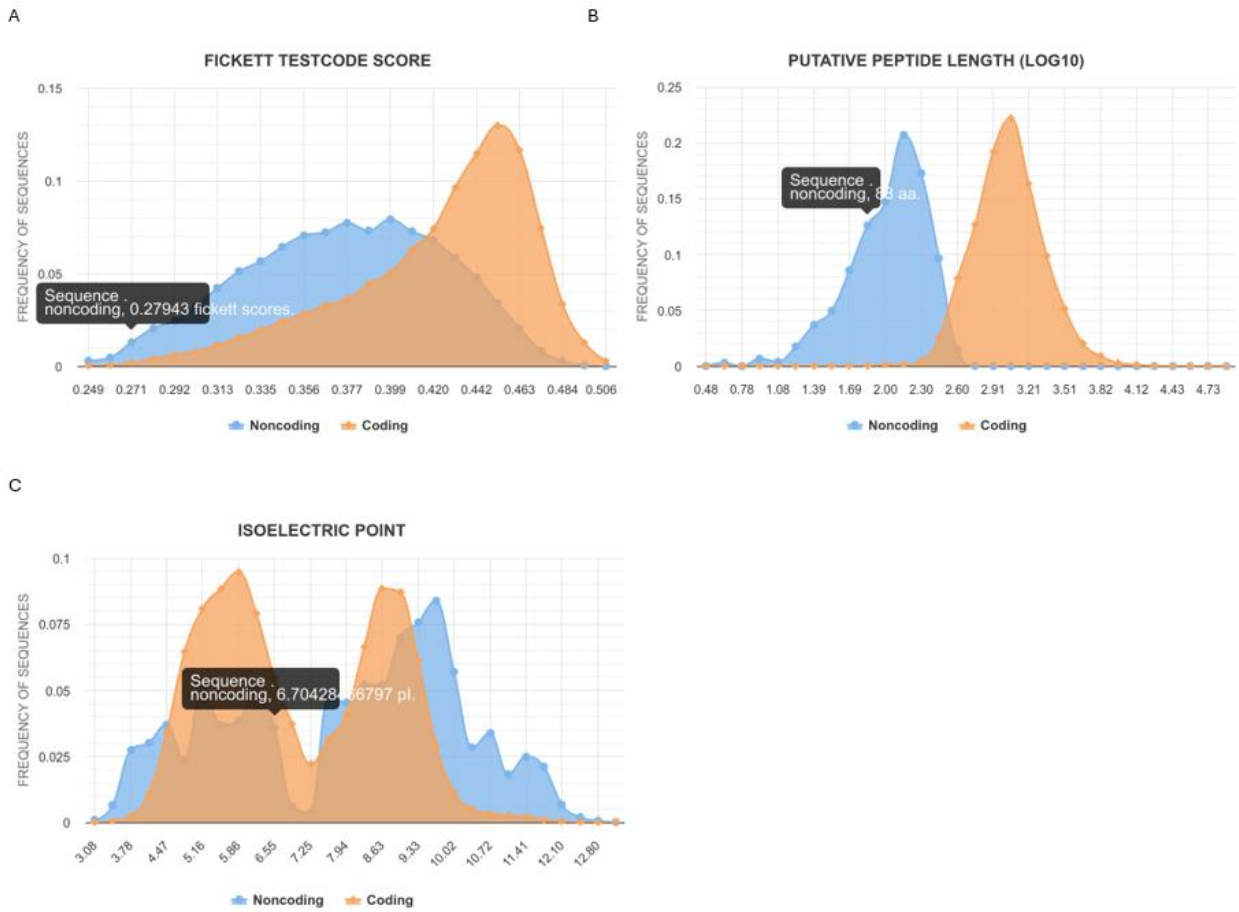

Figure 2. CPC2 results determine the coding potential of sheep MALAT1 and classify it as noncoding sequence. (A) Fickett TESTCODE score was 0.27493, which classifies as a noncoding sequence. (B) The putative peptide length showed 88 amino acids in length. (C) The isoelectric point calculated to be 6.704, which was calculate based on putative ORF.

LncRNA responsiveness to ischemia in fetal sheep islets

LncRNA responsiveness to in vitro ischemia conditions was measured in isolated islets form fetal sheep. Six of the nine lincRNAs were differentially expressed in ischemic conditions compared to optimal culture conditions. Concentrations of MALAT1 and H19 increased with ischemia compared to optimal culture conditions. SI-linc20-39a, LINC28868, SI-linc9-103, and RUNX1T1 Carmen expression decreased with ischemia culture conditions and SI-lin7-41, SI-linc21-42, and SI-lincX27 expressions were unchanged (Figure 3). These data confirm lncRNA expression was responsive to ischemic conditions in fetal sheep islets.

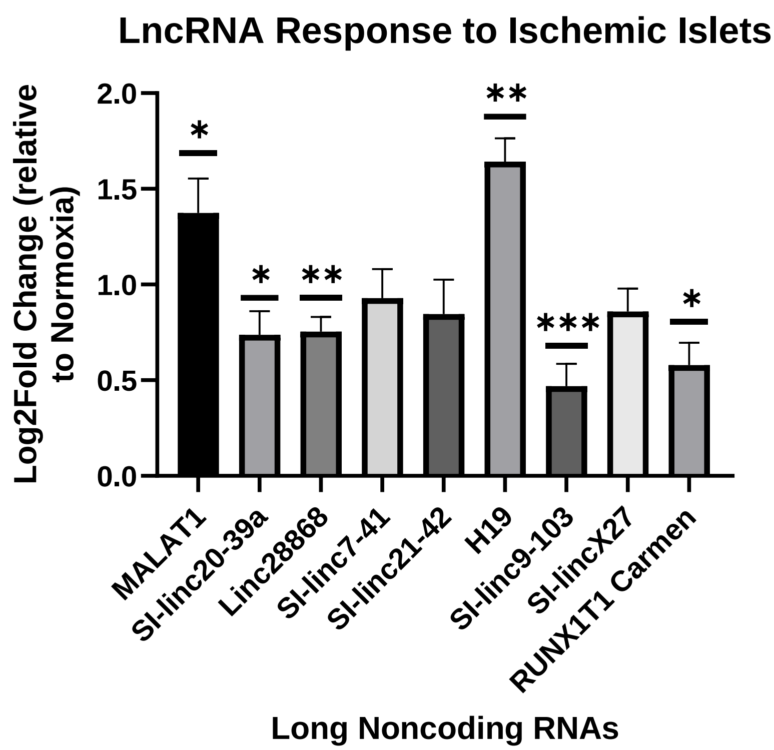

Figure 3. Differentially expressed lncRNAs in ischemic islets.
In vitro ischemic conditions significantly altered 6 of the 9 lncRNAs in pancreatic islets from normal fetal sheep. Among these differentially expressed genes, MALAT1 and H19 concentrations were higher (P<0.05). SI-linc20-39a, LINC28868, SI-linc9-103, and RUNX1T1 Carmen concentrations were lower (P<0.05) with ischemic culture conditions. SI-linc7-41, SI-linc21-42, and SI-lincX27 were not changed. Data analyzed with mixed ANOVA analysis (n = 6), *P<0.05, **P<0.01, ***P<0.001.

Other lncRNAs such as RUNX1T1 Carmen, which is downstream of RUNX1T1, was also classified as a noncoding sequence with 0.348 Fickett score and 57 putative ORF resulting in coding probability to be 0.031 (Table 1). SI-linc9-103 was also a noncoding sequence with 0.358 Fickett Score and 64 amino acids putative ORF. Si-linc20-39a was classified as a noncoding sequence with a Fickett score of 0.358 with ORF of 64 AA and coding probability of 0.084.

LINC28118 (H19) was classified as noncoding sequence with a coding probability of 0.312. On the other hand, LINC28868 overlaps with protein coding gene NUMA1, which is 1.5kbp long. The coding potential yielded a score of 0.387 Fickett score and 261 amino acids putative ORF. SI-linc7-41 and SI-lincX27 were also classified as a coding sequence with a coding probability of 0.968 and 0.998 as shown in Table 1.

Table 1. CPC2 (CPC Version 2.0 standalone package at http://cpc2.cbi.pku.edu.cn/) on lncRNA sequences to determine coding potential. Results were acquired in May 2024.

Islet lincRNA	**Coordinates (LOC_Ram1.02)**	**Coding probability**	**Fickett score**	**Putative peptide length**	**Isoelectric point**	**Label**
SI-linc21-47 (MALAT1)	chr21:45469078-45476376	0.0871836	0.27943	88	6.704	Noncoding
SI-linc20-39a	chr20:39765016-39780849	0.0844073	0.35842	64	8.507	Noncoding
Linc28868	chr15:54659699-54661265	0.999919	0.38729	261	5.908	Coding
SI-linc7-41	chr7:41809092-41911077	0.968046	0.28562	264	8.4402	Coding
LINC28118 (H19)	chr21:45890156-45891071	0.31177	0.46514	90	8.8305	Noncoding
SI-linc9-103	chr9:103899735-103899209	0.0844073	0.35842	64	8.507	Noncoding
SI-linc-X27	X 26053627-26055522	0.997676	0.38613	230	7.880	Coding
RUNX1T1 Carmen	chr9:93919632-93920955	0.0314273	0.34848	57	9.666	noncoding

NF-κB nuclear proteins in MIN6 cells with hypoxia and TNF-α treatment

To investigate NF-kB activity during chronic hypoxia, nuclear NF-κB nuclear abundances were measured by western blot. As shown in Figure 4, the p50 abundances were not different between the 0-hour vs 24-hour hypoxia. TNF-α significantly increased p50 nuclear abundance, and the response was similar between 0 hour and 24-hour hypoxia. p65 nuclear abundance did not differ between 0 hour and 24-hour hypoxia treatment nor did TNF-α stimulated p65 translocation to the nucleus (Figure 5). Hypoxia did not alter NF-κB p50 translocation in the presence of hypoxia but increased with TNF-α stimulation. P65 protein translocation did not respond to hypoxia or TNF-α treatment.

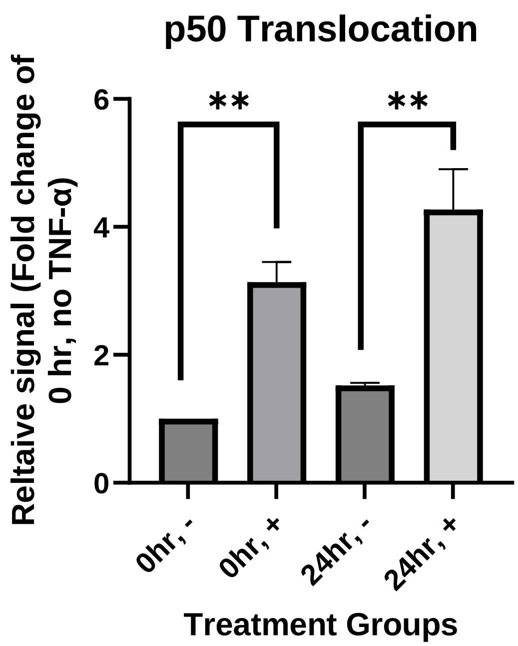

Figure 4. p50 nuclear protein levels in response to hypoxia and TNF-α challenge. MIN6 cells were cultured in hypoxia at 1% O_2 for 24 hours followed by TNF-α treatment for 20 minutes. The p50 subunit protein increases with TNF-alpha treatment. All experiments were performed in biological triplicates and data representative of three independent experiments (n = 3). Data was analyzed with One-way ANOVA followed by Holm-Sidak pairwise comparison, *P<0.05, **P<0.01, ***P<0.001.

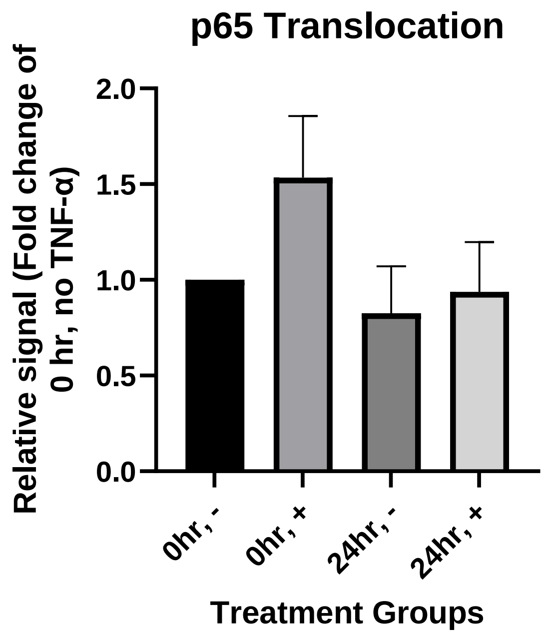

Figure 5. p65 nuclear protein levels in response to hypoxia and TNF-α challenge. Groups were not significantly different in response to hypoxia and TNF-α treatment. All experiments were performed in biological triplicates and data representative of three independent experiments (n = 3). Data was analyzed with One-way ANOVA ($P < 0.05$).

MALAT1 Expression in MIN6 and INS832 cell lines

MALAT1 expression increases in response to ischemic conditions in FGR islets and in ischemic islets, so we decided to mimic chronic hypoxia seen in FGR fetal sheep by measuring MALAT1 expression after 24 hours of hypoxia with 1% O_2 in MIN6 and INS832 cell lines. In Figure 6, in MIN6 cells LDHA mRNA expression marginally increased, and VEGF expression did not differ with hypoxia compared to controls. INS832 cells showed severe cell death and altered mRNA S15 expression in response to hypoxia. Despite the lack of normalization with the hypoxic INS832 cells, there was no difference in MALAT1 expression.

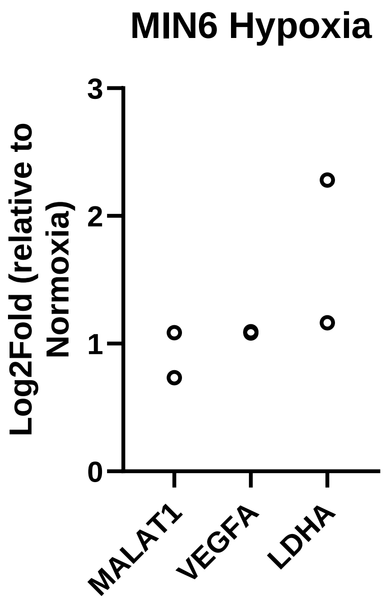

Figure 6. MIN6 cells were incubated in hypoxic gas chambers at 1% O2 for 24 hours followed by RNA isolation and cDNA synthesis (n = 2). LDHA hypoxic gene for one replicate had higher expression by 2.5-folds in response to hypoxia. MALAT1 and VEGFA did not change in response to hypoxia. All experiments were performed in biological triplicates and data representative of two independent experiments (n = 2).

NF-kB response to ischemic conditions in MIN6 and INS832

We used an alternative hypoxia treatment by chemically inducing hypoxia using cobalt (II) chloride ($CoCl_2$). First, a single experiment was conducted to measure the NF-kB response in different concentrations of $CoCl_2$. The concentration was chosen based of least amount of cell death with robust NF-kB luciferase activity. 300 µM $CoCl_2$ increased NF-kB activity compared to 100, 200, so we chose 250 µM, which had no cell death and still exhibited a robust NF-kB response in MIN6 cells. INS832 cells showed some cell death at 300 µM $CoCl_2$ concentrations so 200 µM was chosen for producing robust response in NF-kB activity without substantial cell death that was seen in higher concentrations. Next, we conducted ischemic treatment with low glucose concentrations at 1 mM and 250 µM $CoCl_2$ for MIN6. Experimental groups were control, low glucose (1mM), hypoxia (250µM), and ischemic (250µM $CoCl_2$ and 1mM glucose). In MIN6, there were no significant differences between control and low glucose. Hypoxia increased NF-κB activity but not significantly. Ischemia increased NF-kB activity, whereas low glucose did not affect activity (Figure 7). For INS832, we found no differences across all groups (Figure 8).

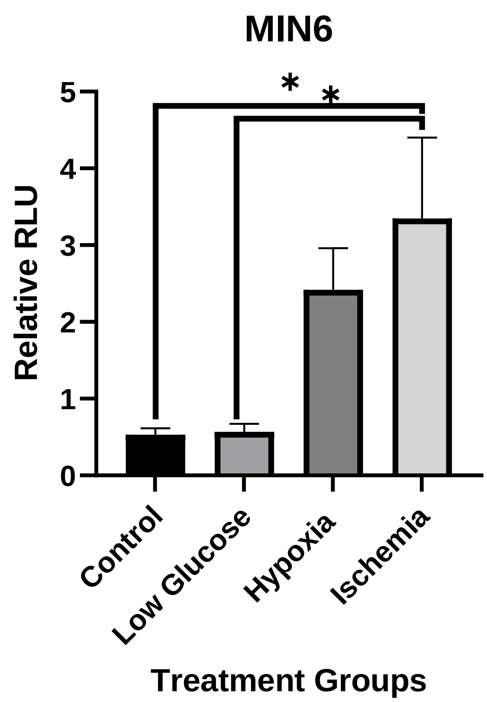

Figure 7. MIN6 cells were incubated in normal, low glucose, hypoxic, and ischemic conditions for 24 hours followed by luciferase assay and BCA (n = 3). NF-kB activity was significantly higher in response to ischemia compared to control and low glucose (P<0.05). In hypoxia, NF-kB activity was increased, but not significantly. Control and low glucose did not differ from each other. All experiments were performed in biological triplicates and data representative of three independent experiments (n = 3). Statistical analysis was done with One-way ANOVA followed by post hoc Tukey test.

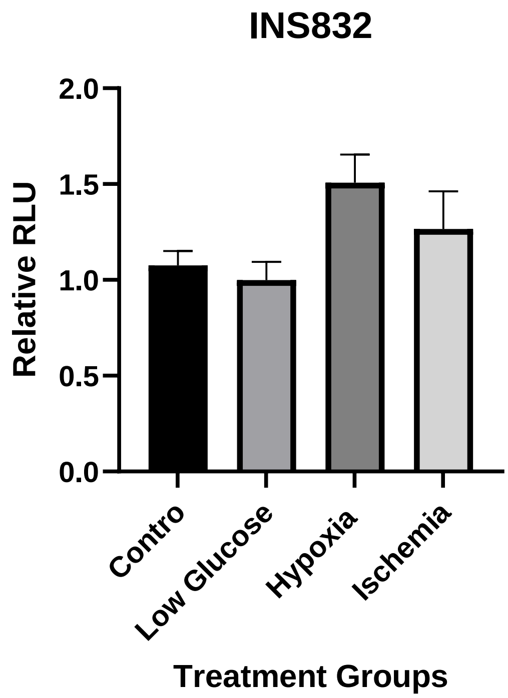

Figure 8. INS832 cells were incubated in normal, low glucose, hypoxic, and ischemic conditions for 24 hours followed by luciferase assay and BCA. All experiments were performed in biological triplicates and data representative of three independent experiments (n = 3). No significant changes in NF-kB activity between groups (One-way ANOVA).

Long noncoding RNAs responsive to hypoxia in oFUVECs

To show 1% O_2 induced a hypoxia response in FUVECs, we measured a hypoxia responsive gene and found increased LDHA expression (Figure 9). The lncRNA genes that were differentially expressed in ischemic islets were also measured in oFUVECs. MALAT1, SI-linc20-39a, LINC28868, SI-linc9-103, and RUNX1T1 Carmen expression were not different in hypoxic oFUVECs compared to cell culture in room air. However, we observed H19 expression increased nearly 7-folds in response to hypoxia (Figure 10). To determine whether there were any changes in NF-kB genes we measured NFKB1 and RELA expression, which were not different (Figure 11).

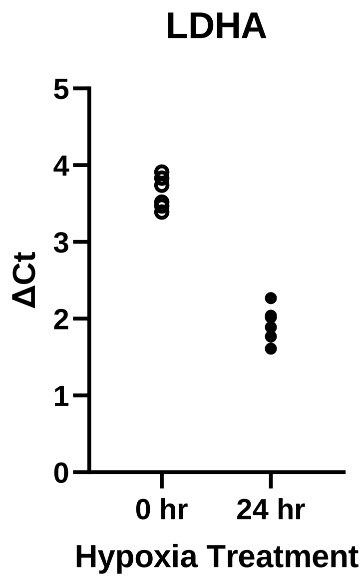

Figure 9. oFUVECs were incubated in hypoxic gas chambers (1% O_2) for 24 hours followed by RNA isolation and cDNA synthesis (n = 6). Data represents each technical replicate (n = 3) for two independent experiments. LDHA expression is higher in response to 24hr hypoxia than 0hr hypoxia.

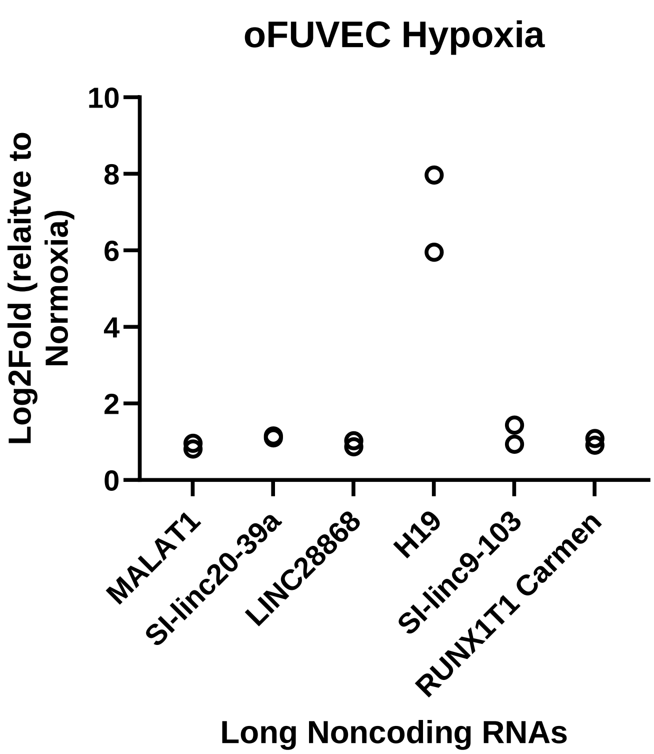

Figure 10. Long noncoding RNAs responsiveness to hypoxia in oFUVECs. oFUVECs were cultured in 1% O_2 for 24 hours (n = 2). MALAT1, SI-linc20-39a, LINC28868, SI-linc9-103, and RUNX1T1 Carmen expression were not much different from normoxia group. H19 expression was increased nearly 7-folds in response to hypoxia.

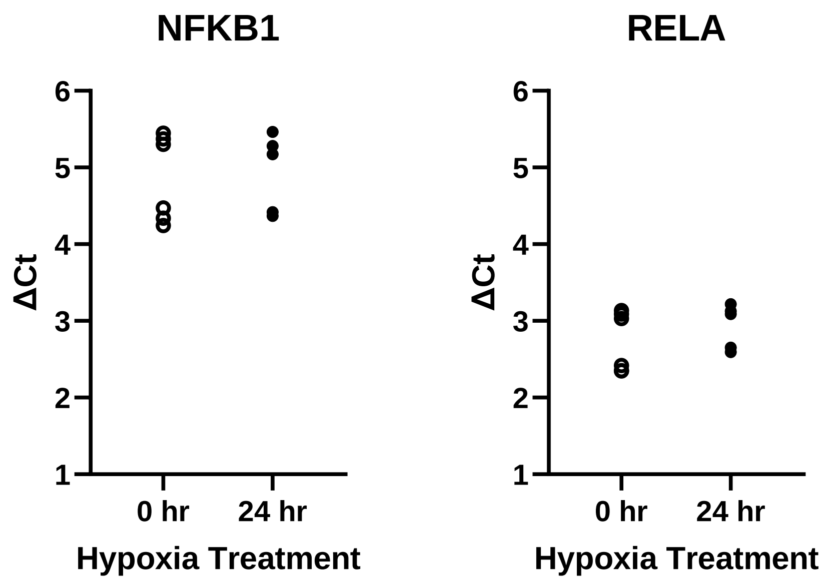

Figure 11. NF-kB expression in response to 24hr hypoxia in oFUVECs. FUVECs were incubated in hypoxic gas chambers (1% O_2) for 24 hours followed by RNA isolation and cDNA synthesis (n = 6). Data represents each technical replicate (n = 3) for two independent experiments. NF-kB genes did not show differences between 0hr and 24hr treated hypoxia in FUVECs.

MALAT1 knockdown with siRNA in oFUVECs

Three MALAT1 siRNAs were generated and pooled to knockdown MALAT1 in primary cells derived from sheep. Mean MALAT1 expression declined 0.55-folds but only 2 replicates were completed (Figure 12). Control and scramble groups were similar.

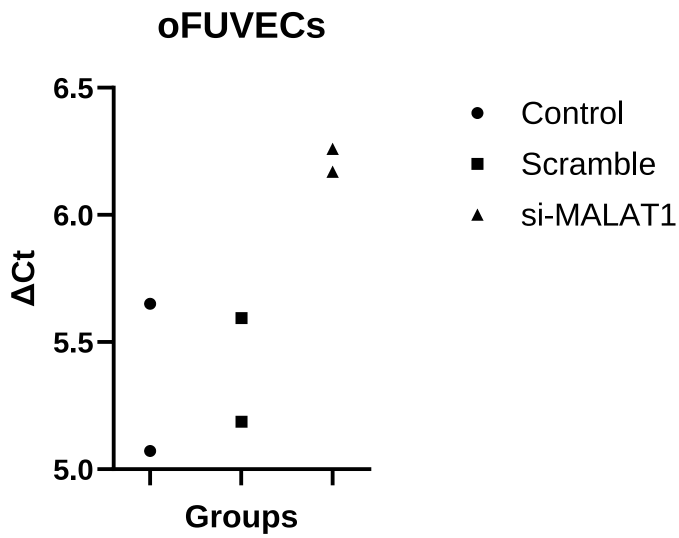

Figure 12. MALAT1 siRNA treated FUVEC cells showed decrease in MALAT1 expression. Si-MALAT1 group decreased to 0.55-folds. All experiments were performed in biological duplicates and data representative of two independent experiments (n = 2).

Discussion

In this study, we determined whether expression of these lncRNAs changed in response to ischemia in primary fetal sheep islets. We found MALAT1 and H19 concentrations increased with ischemia. Previously, MALAT1 expression has been shown to increase in ischemic mice kidneys and in hypoxic cancer cells (Tian et al., 2018; Lelli et al., 2015). However, MALAT1 in ischemic conditions have not been studied in islets and we confirm its response to ischemic fetal sheep islets. Studies have shown H19 expressions to be higher in response to hypoxia and ischemia across various cell types (Wu et al., 2017; Hobuß et al., 2020; Li et al., 2022), which was also seen in fetal ischemic islets. RUNX1T1 Carmen was lower in response to ischemia in fetal sheep islets. CARMEN lncRNA, characterized in humans, has shown to be associated with enhancer elements like MyoD enhancer, and miRNAs that are associated with pluripotency and cardiomyocyte differentiation (Ounzain et al., 2015). It has been characterized to have regulatory roles by mediating cardiovascular cell specification and differentiation by *cis*- and *trans*-epigenetic regulation (Ounzain et al., 2015). Although the role of Carmen in islets is unknown, its potential role in cell differentiation can be investigate in islets from FGR fetuses that have potentially decreased β-cell differentiation (Limesand et al., 2005). Uncharacterized lncRNAs, such as SI-linc20-39a, linc28868 and SI-linc9-103 have also been confirmed to be responsive to ischemia, but more work is needed to determine what roles they have in FGR islets.

To determine the presence of alternative splicing, MALAT1 transcript was sequenced (Figure 1). We did not detect any alternative isoforms of the MALAT1 sequence from islets. Next, the coding potential was determined as a noncoding sequence with short ORF of 88 amino acids. These results indicate that the MALAT1 sequence fits one of the hallmarks of non-protein coding genes with short ORFs. Classes of lncRNAs, such as antisense lncRNAs, have been found to have overlapping sequences with exons and introns of protein coding genes (Ma et al., 2013; Ning et al., 2017). We found other lncRNA predicted sequences were also classified as nonprotein coding sequences with ORFs that ranged from 57 amino acids to 120 amino acids, while LINC28868, SI-linc7-41, and SI-lincX27 had coding potential. The BLAST results showed overlaps of LINC28868 with protein coding gene sequence. LINC28868 contained protein coding regions of NUMA1 201. SI-lincX27 was downstream of a lncRNA (ENSOARG00020015477) but did not show any protein coding gene overlaps. We were able to identify and confirm the coding potential of two novel lncRNAs, SI-linc20-39a and SI-lin9-103, that are differentially expressed in FGR islets and are responsive to ischemia. More work needs to be done to determine what roles these novel lncRNAs have in fetal FGR islets.

To further evaluate MALAT1 in FGR islets, siRNAs were generated to knockdown MALAT1. This was tested in oFUVECs with lipofectamine reagent. Although MALAT1 expression decreased, it was not significant due to small experimental size. Other transfection techniques, such as Siportamine reagent, can be used to knockdown MALAT1 as well. Ultimately, we hope to knockdown MALAT1 in fetal sheep islets. Further studies included testing MALAT1 responsiveness in chronic hypoxia in insulinoma cell lines. Previous studies have shown MALAT1 to be oxygen-dependent in multiple cancer cell lines and primary renal epithelial cells (Lelli et al., 2015). We found that MALAT1 expression did not change in chronically hypoxic MIN6. Hypoxia-inducible genes, such as LDHA and VEGFA, also did not change. Although LDHA increased, it was not a robust response to chronic hypoxia. Therefore, the hypoxia response in MIN6 was limited and may not have been hypoxic enough.

NF-kB translocations were also measured in chronically hypoxic MIN6 cells. We found that INS832 cells resulted in cell death when exposed to chronic hypoxia at 1% O_2. Chronic hypoxia did not change NF-κB subunits, p50 and p65, translocation to the nucleus in MIN6. Although TNF-α stimulation increased p50 translocation, there was no change with 24-hour hypoxia. An alternative method we tried was chemically induced hypoxia using $CoCl_2$. Although we observed hypoxia increase NF-kB activity in MIN6, hypoxic INS832 with $CoCl_2$ did not change NF-κB activity. One study demonstrated a time-course hypoxia (2% O_2) experiment with cytokine induction that showed a decrease in p50 and p65 subunits every two hours up to six hours in porcine islets. Furthermore, nucleus translocation decreased for p65 subunits at 6 hours and 24 hours of hypoxic exposure (Chen et al., 2011). Islets that were treated with TNF-α stimulated p65 translocation and decreased with the duration of hypoxia (Chen et al., 2011). We were unable to replicate these results in the INS832 or MIN6 cell lines. A study conducted a moderate hypoxia treatment on MIN6 and found that 5% O_2 induced activation of cell apoptotic proteins such as Caspase 3 (Sato et al., 2014). 1% O_2 hypoxia may be too low for 24-hour chronic hypoxia. A higher percentage like 2% O_2 or shorter duration should be studied to determine what condition for inducing MALAT1 and hypoxic gene expression in MIN6. In addition, $CoCl_2$-induced hypoxia may be an alternative for inducing MALAT1 expression.

Despite challenges in stimulating MALAT1, we observed increased H19 expression in ischemic islets and hypoxic oFUVECs. In addition, preliminary data has also shown that FGR islets showed a higher expression of H19 (Unpublished). H19 is induced by hypoxia in several studies (Li et al., 2022; Wu et al., 2017). Emerging evidence has shown that H19 lncRNA is associated with islet development, such as β-cell proliferation, in neonatal and postnatal rodents (Sanchez-Parra et al., 2018). They showed that H19 lncRNA has also been shown to be downregulated in islets of newborn rats from low protein fed dams. Further investigations found that H19 knockdown reduced β-cell expansion by reducing β-cell proliferation in vitro (Sanchez-Parra et al., 2018). In addition, fetuses born from low protein diet dams had lower H19 expression and were at risk of developing diabetes due to reduced β-cell mass (Sanchez-Parra et al., 2018). This raises the question of why H19 was upregulated in FGR ischemic fetuses and what are its roles in ischemic islets in the FGR pancreas.

We have confirmed the expression of novel lncRNAs to be responsive in ischemic conditions in fetal sheep islets. Although we failed to establish an in vitro model using insulinoma cells lines to further define what potential regulatory roles MALAT1 has on FGR islets, we were able to generate siRNAs knockdown MALAT1 in sheep endothelial cells. Primary islets may be the ideal in vitro model to investigate the regulatory roles of lncRNA in fetal FGR islets under hypoxic and ischemic conditions. The limitations for this project include small experimental replicates and lack of stable reference genes. YWHAZ and TBP transcripts changed in response to ischemia and only S15 abundance was expressed stably. Working with primary fetal sheep islets may have limitations due to limited availability, inability to expand in vitro cell culture, and there are currently no immortalized sheep β-cell line. In addition, further validation for efficiency of siRNA knockdown of MALAT1 is required, and this includes testing various concentrations of siRNA to optimize MALAT1 knockdown. Future experiments will include loss of function experiments such as MALAT1 knockdown in primary islets in hypoxic environments.

NF-kB expression and translocation can be evaluated with loss of MALAT1 knockdown. NF-kB activity can also be evaluated with adenovirus luciferase transfection followed by MALAT1 knockdown.

References

1. Acharya, G., Wilsgaard, T., Rosvold Berntsen, G. K., Maltau, J. M., & Kiserud, T. (2006). Umbilical vein constriction at the umbilical ring: a longitudinal study. *Ultrasound in Obstetrics and Gynecology*, 28(2), 150-155. doi: 10.1002/uog.2711. PMID: 16691633.
2. Aguilera, N., Salas-Pérez, F., Ortíz, M., Álvarez, D., Echiburú, B., & Maliqueo, M. (2022). Rodent models in placental research. Implications for fetal origins of adult disease. *Animal Reproduction*, *19*(1), e20210134. doi: 10.1590/1984-3143-AR2021-0134. PMID: 35493783; PMCID: PMC9037606.
3. Ahlgren, U., Jonsson, J., Jonsson, L., Simu, K., & Edlund, H. (1998). β-Cell-specific inactivation of the mouseIpf1/Pdx1 gene results in loss of the β-cell phenotype and maturity onset diabetes. *Genes & development*, *12*(12), 1763-1768. doi: 10.1101/gad.12.12.1763. PMID: 9637677; PMCID: PMC316911.
4. Akerman I, Tu Z, Beucher A, Rolando DMY, Sauty-Colace C, Benazra M, Nakic N, Yang J, Wang H, Pasquali L, Moran I, Garcia-Hurtado J, Castro N, Gonzalez-Franco R, Stewart AF, Bonner C, Piemonti L, Berney T, Groop L, Kerr-Conte J, Pattou F, Argmann C, Schadt E, Ravassard P, Ferrer J. (2014). Human Pancreatic β Cell lncRNAs Control Cell-Specific Regulatory Networks. *Cell metabolism*, *25*(2), 400-411. doi: 10.1016/j.cmet.2016.11.016. PMID: 28041957; PMCID: PMC5300904.
5. Arnes, L., Akerman, I., Balderes, D. A., Ferrer, J., & Sussel, L. (2016). βlinc1 encodes a long noncoding RNA that regulates islet β-cell formation and function. *Genes & development*, *30*(5), 502-507. doi: 10.1101/gad.273821.115. PMID: 26944677; PMCID: PMC4782045.
6. Barry, J. S., Rozance, P. J., & Anthony, R. V. (2008, June). An animal model of placental insufficiency-induced intrauterine growth restriction. *In Seminars in perinatology* (Vol. 32, No. 3, pp. 225-230). WB Saunders. doi: 10.1053/j.semperi.2007.11.004. PMID: 18482626.
7. Bell AW, Wilkening RB, Meschia G. (1987). Some aspects of placental function in chronically heat-stressed ewes. *Journal of Developmental Physiology, 9*(1):17-29. PMID: 3559063.
8. Bell A.W., McBride B. W., Slepetis R., Early R. J, Currie W.B. (1989). Chronic Heat Stress and Prenatal Development in Sheep: I. Conceptus Growth and Maternal Plasma Hormones and Metabolites, *Journal of Animal Science*, 67:12, 3289–3299, https://doi.org/10.2527/jas1989.67123289x.
9. Béringue, F., Blondeau, B., Castellotti, M. C., Bréant, B., Czernichow, P., & Polak, M. (2002). Endocrine pancreas development in growth-retarded human fetuses. *Diabetes*, *51*(2), 385-391. doi:10.2337/diabetes.51.2.385.
10. Bernard D, Prasanth KV, Tripathi V, Colasse S, Nakamura T, Xuan Z, Zhang MQ, Sedel F, Jourdren L, Coulpier F, Triller A, Spector DL, Bessis A. (2010). A long nuclear-retained non-coding RNA regulates synaptogenesis by modulating gene expression. *The EMBO*

Journal, *29*(18):3082-93. doi: 10.1038/emboj.2010.199. PMID: 20729808; PMCID: PMC2944070.

11. Bonner-Weir, S., Aguayo-Mazzucato, C., & Weir, G. C. (2016). Dynamic development of the pancreas from birth to adulthood. *Upsala journal of medical sciences*, *121*(2), 155-158. PMID: 26998806; PMCID: PMC4900072.
12. Brown, L. D., Rozance, P. J., Wang, D., Eroglu, E. C., Wilkening, R. B., Solmonson, A., & Wesolowski, S. R. (2024). Increased hepatic glucose production with lower oxidative metabolism in the growth-restricted fetus. *JCI insight*, 9(10). doi: 10.1172/jci.insight.176497. PMID: 38687612; PMCID: PMC11141920.
13. Chen, C., Moreno, R., Samikannu, B., Bretzel, R. G., Schmitz, M. L., & Linn, T. (2011). Improved intraportal islet transplantation outcome by systemic IKK-beta inhibition: NF-κB activity in pancreatic islets depends on oxygen availability. *American Journal of Transplantation*, 11(2), 215-224. doi: 10.1111/j.1600-6143.2010.03390.x. Epub 2011 Jan 10. PMID: 21219576.
14. Chew, L. C., & Verma, R. P. (2020). Fetal growth restriction. PMID: 32965939.
15. Colella, M., Frérot, A., Novais, A. R., & Baud, O. (2018). Neonatal and long-term consequences of fetal growth restriction. *Current pediatric reviews, 14*(4), 212-218. doi: 10.2174/1573396314666180712114531. PMID: 29998808; PMCID: PMC6416241.
16. Constância, M., Hemberger, M., Hughes, J., Dean, W., Ferguson-Smith, A., Fundele, R., ... & Reik, W. (2002). Placental-specific IGF-II is a major modulator of placental and fetal growth. *Nature, 417*(6892), 945-948. doi: 10.1038/nature00819. PMID: 12087403.
17. Darby, J. R., Varcoe, T. J., Orgeig, S., & Morrison, J. L. (2020). Cardiorespiratory consequences of intrauterine growth restriction: Influence of timing, severity and duration of hypoxaemia. *Theriogenology*, 150, 84-95. doi: 10.1016/j.theriogenology.2020.01.080. PMID: 32088029.
18. Dilworth, M. R., Kusinski, L. C., Cowley, E., Ward, B. S., Husain, S. M., Constancia, M., ... & Glazier, J. D. (2010). Placental-specific Igf2 knockout mice exhibit hypocalcemia and adaptive changes in placental calcium transport. *Proceedings of the National Academy of Sciences, 107*(8), 3894-3899. doi: 10.1073/pnas.0911710107. PMID: 20133672; PMCID: PMC2840526.
19. Ding, H., Wang, F., Shi, X., Ma, H., Du, Y., Hou, L., & Xing, N. (2020). LncRNA MALAT1 induces the dysfunction of β cells via reducing the histone acetylation of the PDX-1 promoter in type 1 diabetes. *Experimental and molecular pathology*, *114*, 104432. doi: 10.1016/j.yexmp.2020.104432. PMID: 32243891.
20. Flamant, L., Toffoli, S., Raes, M., & Michiels, C. (2009). Hypoxia regulates inflammatory gene expression in endothelial cells. *Experimental cell research*, 315(5), 733-747. doi: 10.1016/j.yexcr.2008.11.020. Epub 2008 Dec 7. PMID: 19101540.
21. Fowden, A. L., & Hay Jr, W. W. (1988). The effects of pancreatectomy on the rates of glucose utilization, oxidation and production in the sheep fetus. *Quarterly Journal of Experimental Physiology: Translation and Integration*, *73*(6), 973-984. doi: 10.1113/expphysiol.1988.sp003231. PMID: 3070626.

22. Fowden, A. L. (1992). The role of insulin in fetal growth. *Early human development*, 29(1-3), 177-181. https://doi.org/10.1016/0378-3782(92)90135-4.
23. Fowden, A. L., Hughes, P., & Comline, R. S. (1989). The effects of insulin on the growth rate of the sheep fetus during late gestation. *Quarterly Journal of Experimental Physiology: Translation and Integration, 74*(5), 703-714. doi: 10.1113/expphysiol.1989.sp003322. PMID: 2687925.
24. Frantz, E. D. C., Aguila, M. B., da Rocha Pinheiro-Mulder, A., & Mandarim-de-Lacerda, C. A. (2011). Transgenerational endocrine pancreatic adaptation in mice from maternal protein restriction in utero. *Mechanisms of ageing and development, 132*(3), 110-116. doi: 10.1016/j.mad.2011.01.003. Epub 2011 Feb 1. PMID: 21291904.
25. Galan, H. L., Anthony, R. V., Rigano, S., Parker, T. A., de Vrijer, B., Ferrazzi, E., ... & Regnault, T. R. (2005). Fetal hypertension and abnormal Doppler velocimetry in an ovine model of intrauterine growth restriction. *American journal of obstetrics and gynecology*, 192(1), 272-279. doi: 10.1016/j.ajog.2004.05.088. PMID: 15672036.
26. Green, A. S., Rozance, P. J., & Limesand, S. W. (2010). Consequences of a compromised intrauterine environment on islet function. *The Journal of endocrinology*, 205(3), 211. PMID: 20223861; PMCID: PMC3526069.
27. Greenough, A., Nicolaides, K. H., & Lagercrantz, H. (1990). Human fetal sympathoadrenal responsiveness. *Early Human Development*, *23*(1), 9-13. doi.org/10.1016/0378-3782(90)90124-2.
28. Harmon, E. B., Apelqvist, A. A., Smart, N. G., Gu, X., Osborne, D. H., & Kim, S. K. (2004). GDF11 modulates NGN3+ islet progenitor cell number and promotes β-cell differentiation in pancreas development. *Development*, 131(24):6163-74. doi: 10.1242/dev.01535. Epub 2004 Nov 17. PMID: 15548585.
29. Hay, W. W., Meznarich, H. K., Digiacomo, J. E., Hirst, K., & Zerbe, G. (1988). Effects of insulin and glucose concentrations on glucose utilization in fetal sheep. *Pediatric Research*, *23*(4), 381-387. doi: 10.1203/00006450-198804000-00008. PMID: 3287321.
30. Hellerström, C., & Swenne, I. (1991). Functional maturation and proliferation of fetal pancreatic β-cells. *Diabetes*, 40 (Supplement_2), 89-93. doi: 10.2337/diab.40.2.s89. PMID: 1748274.
31. Hobuß, L., Foinquinos, A., Jung, M., Kenneweg, F., Xiao, K., Wang, Y., ... & Thum, T. (2020). Pleiotropic cardiac functions controlled by ischemia-induced lncRNA H19. Journal of *Molecular and Cellular Cardiology*, 146, 43-59. doi: 10.1016/j.yjmcc.2020.07.001. Epub 2020 Jul 8. PMID: 32649928.
32. Hutchinson JN, Ensminger AW, Clemson CM, Lynch CR, Lawrence JB, Chess A. (2007). A screen for nuclear transcripts identifies two linked noncoding RNAs associated with SC35 splicing domains. *BMC Genomics.* 1;8:39. doi: 10.1186/1471-2164-8-39. PMID: 17270048; PMCID: PMC1800850.
33. Jabary, M., Onoda, A., Kitase, Y. *et al.* Fetal growth restriction followed by early catch-up growth impairs pancreatic islet morphology in male rats. *Sci Rep* **13**, 2732 (2023). https://doi.org/10.1038/s41598-023-28584-2.

34. Jensen, C. B., Storgaard, H., Dela, F., Holst, J. J., Madsbad, S., & Vaag, A. A. (2002). Early differential defects of insulin secretion and action in 19-year-old Caucasian men who had low birth weight. *Diabetes*, *51*(4), 1271-1280. PMID: 11916955.
35. Ji P, Diederichs S, Wang W, Böing S, Metzger R, Schneider PM, Tidow N, Brandt B, Buerger H, Bulk E, Thomas M, Berdel WE, Serve H, Müller-Tidow C. (2003). MALAT-1, a novel noncoding RNA, and thymosin beta4 predict metastasis and survival in early-stage non-small cell lung cancer. *Oncogene*. *22*(39):8031-41. doi: 10.1038/sj.onc.1206928. PMID: 12970751.
36. Kaijser, M., Edstedt Bonamy, A. K., Akre, O., Cnattingius, S., Granath, F., Norman, M., & Ekbom, A. (2009). Perinatal risk factors for diabetes in later life. *Diabetes*, *58*(3), 523-526. doi: 10.2337/db08-0558. Epub 2008 Dec 9. PMID: 19066311; PMCID: PMC2646049.
37. Kamphof, H. D., Posthuma, S., Gordijn, S. J., & Ganzevoort, W. (2022). Fetal growth restriction: mechanisms, epidemiology, and management. *Maternal-Fetal Medicine*, *4*(03), 186-196. DOI: 10.1097/FM9.0000000000000161.
38. Kanasaki M, Srivastava SP, Yang F, Xu L, Kudoh S, Kitada M, Ueki N, Kim H, Li J, Takeda S, Kanasaki K, Koya D. Deficiency in catechol-o-methyltransferase is linked to a disruption of glucose homeostasis in mice. *Scientific Reports*. 2017 Aug 11;7(1):7927. doi: 10.1038/s41598-017-08513-w. PMID: 28801594; PMCID: PMC5554180.
39. Kelly, A. C., Bidwell, C. A., McCarthy, F. M., Taska, D. J., Anderson, M. J., Camacho, L. E., & Limesand, S. W. (2017). RNA sequencing exposes adaptive and immune responses to intrauterine growth restriction in fetal sheep islets. *Endocrinology*, *158*(4), 743-755. doi: 10.1210/en.2016-1901. PMID: 28200173; PMCID: PMC5460795.
40. Kumar, M., & Goyal, R. (2017). LncRNA as a therapeutic target for angiogenesis. *Current topics in medicinal chemistry*, *17*(15), 1750-1757. doi: 10.2174/1568026617666161116144744. PMID: 27848894; PMCID: PMC5421140.
41. Lelli A, Nolan KA, Santambrogio S, Gonçalves AF, Schönenberger MJ, Guinot A, Frew IJ, Marti HH, Hoogewijs D, Wenger RH. (2015). Induction of long noncoding RNA MALAT1 in hypoxic mice. *Hypoxia* (Auckl). 3:45-52. doi: 10.2147/HP.S90555. PMID: 27774481; PMCID: PMC5045088.
42. Leos, R. A., Anderson, M. J., Chen, X., Pugmire, J., Anderson, K. A., & Limesand, S. W. (2010). Chronic exposure to elevated norepinephrine suppresses insulin secretion in fetal sheep with placental insufficiency and intrauterine growth restriction. *American Journal of Physiology-Endocrinology and Metabolism, 298*(4), E770-E778. doi: 10.1152/ajpendo.00494.2009. PMID: 20086198; PMCID: PMC2853210.
43. Li, H., Wang, J., Jin, Y., Lin, J., Gong, L., & Xu, Y. (2022). Hypoxia upregulates the expression of lncRNA H19 in non-small cell lung cancer cells and induces drug resistance. Translational Cancer Research, 11(8), 2876.
44. Limesand, S. W., & Hay Jr, W. W. (2003). Adaptation of ovine fetal pancreatic insulin secretion to chronic hypoglycaemia and euglycaemic correction. The Journal of physiology, 547(1), 95-105. doi: 10.1113/jphysiol.2002.026831. Epub 2002 Oct 4. PMID: 12562941; PMCID: PMC2342612.

45. Limesand, S. W., Jensen, J., Hutton, J. C., & Hay Jr, W. W. (2005). Diminished β-cell replication contributes to reduced β-cell mass in fetal sheep with intrauterine growth restriction. American Journal of Physiology-Regulatory, Integrative and Comparative *Physiology, 288*(5), R1297-R1305. doi: 10.1152/ajpregu.00494.2004. PMID: 15650129.
46. Limesand, S. W., Rozance, P. J., Zerbe, G. O., Hutton, J. C., & Hay, W. W. (2006). Attenuated insulin release and storage in fetal sheep pancreatic islets with intrauterine growth restriction. *Endocrinology, 147*(3), 1488-1497. doi: 10.1210/en.2005-0900. PMID: 16339204.
47. Limesand, S. W., Rozance, P. J., Smith, D., & Hay Jr, W. W. (2007). Increased insulin sensitivity and maintenance of glucose utilization rates in fetal sheep with placental insufficiency and intrauterine growth restriction. *American Journal of Physiology-Endocrinology and Metabolism, 293*(6), E1716-E1725. doi: 10.1152/ajpendo.00459.2007. PMID: 17895285.
48. Limesand, S. W., Rozance, P. J., Macko, A. R., Anderson, M. J., Kelly, A. C., & Hay Jr, W. W. (2013). Reductions in insulin concentrations and β-cell mass precede growth restriction in sheep fetuses with placental insufficiency. *American Journal of Physiology-Endocrinology and Metabolism, 304*(5), E516-E523. doi: 10.1152/ajpendo.00435.2012. PMID: 23277186; PMCID: PMC3602661.
49. Limesand, S. W., Camacho, L. E., Kelly, A. C., & Antolic, A. T. (2018). Impact of thermal stress on placental function and fetal physiology. *Animal Reproduction, 15*(Suppl 1), 886. doi: 10.21451/1984-3143-AR2018-0056. PMID: 36249845; PMCID: PMC9536067.
50. Liu, Q., & Li, B. (2021). The diagnostic value of ultrasound detection of the fetal middle cerebral artery, umbilical artery blood flow and fetal movement reduction in fetal distress. *American journal of translational research, 13*(4), 3529. PMID: 34017532; PMCID: PMC8129210.
51. Ma, L., Bajic, V. B., & Zhang, Z. (2013). On the classification of long non-coding RNAs. *RNA biology*, 10(6), 924-933. PMID: 23696037; PMCID: PMC4111732.
52. Macko, A. R., Yates, D. T., Chen, X., Green, A. S., Kelly, A. C., Brown, L. D., & Limesand, S. W. (2013). Elevated plasma norepinephrine inhibits insulin secretion, but adrenergic blockade reveals enhanced β-cell responsiveness in an ovine model of placental insufficiency at 0.7 of gestation. *Journal of Developmental Origins of Health and Disease, 4*(5), 402-410. doi: 10.1017/S2040174413000093. PMID: 24358443; PMCID: PMC3864835.
53. Melloul, D. (2004). Transcription factors in islet development and physiology: role of PDX-1 in beta-cell function. *Annals of the New York Academy of Sciences*, *1014*(1), 28-37. doi: 10.1196/annals.1294.003. PMID: 15153417.
54. Meschia, G., Makowski, E. L., & Battaglia, F. C. (1969). The use of indwelling catheters in the uterine and umbilical veins of sheep for a description of fetal acid-base balance and oxygenation. The Yale Journal of Biology and Medicine, 42(3-4), 154. PMID: 5371158; PMCID: PMC2593490.

55. Michalik KM, You X, Manavski Y, Doddaballapur A, Zörnig M, Braun T, John D, Ponomareva Y, Chen W, Uchida S, Boon RA, Dimmeler S. (2014). Long noncoding RNA MALAT1 regulates endothelial cell function and vessel growth. *Circulation Research*. *114*(9):1389-97. doi: 10.1161/CIRCRESAHA.114.303265. PMID: 24602777.
56. Milovanovic, I., Njuieyon, F., Deghmoun, S., Chevenne, D., Levy-Marchal, C., & Beltrand, J. (2014). SGA children with moderate catch-up growth are showing the impaired insulin secretion at the age of 4. *PloS one*, *9*(6), e100337. doi: 10.1371/journal.pone.0100337. PMID: 24979613; PMCID: PMC4076235.
57. Miralles, F., Philippe, P., Czernichow, P., & Scharfmann, R. (1998). Expression of nerve growth factor and its high-affinity receptor Trk-A in the rat pancreas during embryonic and fetal life. *Journal of endocrinology*, *156*(3), 431-439. doi: 10.1677/joe.0.1560431. PMID: 9582499.
58. Morán I, Akerman I, van de Bunt M, Xie R, Benazra M, Nammo T, Arnes L, Nakić N, García-Hurtado J, Rodríguez-Seguí S, Pasquali L, Sauty-Colace C, Beucher A, Scharfmann R, van Arensbergen J, Johnson PR, Berry A, Lee C, Harkins T, Gmyr V, Pattou F, Kerr-Conte J, Piemonti L, Berney T, Hanley N, Gloyn AL, Sussel L, Langman L, Brayman KL, Sander M, McCarthy MI, Ravassard P, Ferrer J. (2012). Human β cell transcriptome analysis uncovers lncRNAs that are tissue-specific, dynamically regulated, and abnormally expressed in type 2 diabetes. *Cell Metabolism, 16*(4):435-48. doi: 10.1016/j.cmet.2012.08.010. PMID: 23040067; PMCID: PMC3475176.
59. Motterle, A., Gattesco, S., Peyot, M. L., Esguerra, J. L. S., Gomez-Ruiz, A., Laybutt, D. R., ... & Regazzi, R. (2017). Identification of islet-enriched long non-coding RNAs contributing to β-cell failure in type 2 diabetes. *Molecular metabolism*, *6*(11), 1407-1418. doi: 10.1016/j.molmet.2017.08.005. PMID: 29107288; PMCID: PMC5681241.
60. Nardozza, L. M. M., Caetano, A. C. R., Zamarian, A. C. P., Mazzola, J. B., Silva, C. P., Marçal, V. M. G., ... & Araujo Júnior, E. (2017). Fetal growth restriction: current knowledge. *Archives of gynecology and obstetrics*, *295*, 1061-1077. doi: 10.1007/s00404-017-4341-9. Epub 2017 Mar 11. PMID: 28285426.
61. Nicolini, U., Hubinont, C. J., Santolaya, J., Fisk, N. M., & Rodeck, C. H. (1990). Effects of fetal intravenous glucose challenge in normal and growth retarded fetuses. *Hormone and Metabolic Research*, *22*(08), 426-430. doi: 10.1055/s-2007-1004939. PMID: 2227801.
62. Nieto-Diaz, A., Villar, J., Matorras-Weinig, R., & Valenzuela-Ruiz, P. (1996). Intrauterine growth retardation at term: association between anthropometric and endocrine parameters. *Acta obstetricia et gynecologica Scandinavica, 75(*2), 127-131. doi: 10.3109/00016349609033303. PMID: 8604597.
63. Ning, Q., Li, Y., Wang, Z., Zhou, S., Sun, H., & Yu, G. (2017). The evolution and expression pattern of human overlapping lncRNA and protein-coding gene pairs. Scientific reports, 7(1), 42775. doi: 10.1038/srep42775. PMID: 28344339; PMCID: PMC5366806.

64. Norlin, S., Ahlgren, U., & Edlund, H. (2005). Nuclear factor-κB activity in β-cells is required for glucose-stimulated insulin secretion. *Diabetes*, 54(1), 125-132. https://doi.org/10.2337/diabetes.54.1.125.
65. Oeckinghaus A, Hayden MS, Ghosh S. (2011). Crosstalk in NF-κB signaling pathways. *Nature Immunology*. 12(8):695-708. doi: 10.1038/ni.2065. PMID: 21772278.
66. Osuchukwu, O. O., & Reed, D. J. (2020). Small for gestational age.
67. Pardi, G., Cetin, I., Marconi, A. M., Lanfranchi, A., Bozzetti, P., Farrazzi, E., ... & Battaglia, F. C. (1993). Diagnostic value of blood sampling in fetuses with growth retardation. *New England Journal of Medicine, 328*(10), 692-696. doi: 10.1056/NEJM199303113281004. PMID: 8433728.
68. Ounzain, S., Micheletti, R., Arnan, C., Plaisance, I., Cecchi, D., Schroen, B., ... & Pedrazzini, T. (2015). CARMEN, a human super enhancer-associated long noncoding RNA controlling cardiac specification, differentiation and homeostasis. *Journal of molecular and cellular cardiology*, 89, 98-112. doi: 10.1016/j.yjmcc.2015.09.016. Epub 2015 Sep 28. PMID: 26423156.
69. Phipps, K., Barker, D. J. P., Hales, C. N., Fall, C. H. D., Osmond, C., & Clark, P. M. S. (1993). Fetal growth and impaired glucose tolerance in men and women. *Diabetologia*, *36*, 225-228. doi: 10.1007/BF00399954. PMID: 8462770.
70. Pierucci, D., Cicconi, S., Bonini, P., Ferrelli, F., Pastore, D., Matteucci, C., Marselli L, Marchetti P, Ris F, Halban P, Oberholzer J, Federici M, Cozzolino F, Lauro R, Borboni P, & Marlier, L. N. J. L. (2001). NGF-withdrawal induces apoptosis in pancreatic beta cells in vitro. *Diabetologia*, *44*, 1281-1295. doi: 10.1007/s001250100650. PMID: 11692177.
71. Radford, B. N., & Han, V. K. M. (2019). Offspring from maternal nutrient restriction in mice show variations in adult glucose metabolism similar to human fetal growth restriction. *Journal of Developmental Origins of Health and Disease, 10(*4), 469-478. doi: 10.1017/S2040174418000983. Epub 2018 Dec 3. PMID: 30501657.
72. Regnault, T. R. H., Galan, H. L., Parker, T. A., & Anthony, R. V. (2002). Placental development in normal and compromised pregnancies—a review. *Placenta, 23*, S119-S129. doi: 10.1053/plac.2002.0792. PMID: 11978069.
73. Regnault, T. R. H. (2003). Ruminant models of prenatal growth restriction. *Reproduction, 61*(5689), 183-194. PMID: 14635935.
74. Regnault, T. R. H., de Vrijer, B., Galan, H. L., Wilkening, R. B., Battaglia, F. C., & Meschia, G. (2007). Development and mechanisms of fetal hypoxia in severe fetal growth restriction. *Placenta, 28(*7), 714-723. doi: 10.1016/j.placenta.2006.06.007. PMID: 16962658.
75. Reynolds LP, Ferrell CL, Nienaber JA, Ford SP. (1985). Effects of chronic environmental heat stress on blood flow and nutrient uptake of the gravid bovine uterus and foetus. *The Journal of Agricultural Science*. 104(2):289-297. doi:10.1017/S002185960004394X.
76. Reynolds, L. P., Caton, J. S., Redmer, D. A., Grazul-Bilska, A. T., Vonnahme, K. A., Borowicz, P. P., ... & Spencer, T. E. (2006). Evidence for altered placental blood flow and vascularity

in compromised pregnancies. *The Journal of physiology, 572*(1), 51-58. doi: 10.1113/jphysiol.2005.104430. 16469783; PMCID: PMC1779650.

77. Rigano, S., Bozzo, M., Ferrazzi, E., Bellotti, M., Battaglia, F. C., & Galan, H. L. (2001). Early and persistent reduction in umbilical vein blood flow in the growth-restricted fetus: a longitudinal study. *American journal of obstetrics and gynecology*, 185(4), 834-838. doi: 10.1067/mob.2001.117356. PMID: 11641661.
78. Rozance, P. J., Anderson, M., Martinez, M., Fahy, A., Macko, A. R., Kailey, J., Seedorf GJ, Abman SH, Hay WW Jr, & Limesand, S. W. (2015). Placental insufficiency decreases pancreatic vascularity and disrupts hepatocyte growth factor signaling in the pancreatic islet endothelial cell in fetal sheep. *Diabetes*, *64*(2), 555-564. doi: 10.2337/db14-0462. Epub 2014 Sep 23. PMID: 25249573; PMCID: PMC4303968.
79. Rueda-Clausen, C. F., Stanley, J. L., Thambiraj, D. F., Poudel, R., Davidge, S. T., & Baker, P. N. (2014). Effect of prenatal hypoxia in transgenic mouse models of preeclampsia and fetal growth restriction. *Reproductive Sciences, 21*, 492-502. doi: 10.1177/1933719113503401. PMID: 24084523; PMCID: PMC3960835.
80. Xiong, L., Gong, Y., Wu, L., Li, J., He, W., Zhu, X., & Xiao, H. (2020). LncRNA-Malat1 is involved in lipotoxicity-induced ß-cell dysfunction and the therapeutic effect of exendin-4 via Ptbp1. *Endocrinology*, 161(7), bqaa065. doi: 10.1210/endocr/bqaa065. PMID: 32324218.
81. Sanchez-Parra, C., Jacovetti, C., Dumortier, O., Lee, K., Peyot, M. L., Guay, C., ... & Regazzi, R. (2018). Contribution of the long noncoding RNA H19 to β-cell mass expansion in neonatal and adult rodents. *Diabetes*, 67(11), 2254-2267. doi: 10.2337/db18-0201. Epub 2018 Aug 16. PMID: 30115652.
82. Sato, Y., Inoue, M., Yoshizawa, T., & Yamagata, K. (2014). Moderate hypoxia induces β-cell dysfunction with HIF-1–independent gene expression changes. PLoS One, 9(12), e114868. doi: 10.1371/journal.pone.0114868. PMID: 25503986; PMCID: PMC4264765.
83. Schmitz, S. U., Grote, P., & Herrmann, B. G. (2016). Mechanisms of long noncoding RNA function in development and disease. *Cellular and molecular life sciences*, *73*, 2491-2509. PMID: 27007508; PMCID: PMC4894931.
84. Senée, V., Chelala, C., Duchatelet, S., Feng, D., Blanc, H., Cossec, J. C., ... & Julier, C. (2006). Mutations in GLIS3 are responsible for a rare syndrome with neonatal diabetes mellitus and congenital hypothyroidism. *Nature genetics*, 38(6), 682-687. doi: 10.1038/ng1802. PMID: 16715098.
85. Simmons, R. A., Templeton, L. J., & Gertz, S. J. (2001). Intrauterine growth retardation leads to the development of type 2 diabetes in the rat. *Diabetes, 50*(10), 2279-2286. doi: 10.2337/diabetes.50.10.2279. PMID: 11574409.
86. Smart, N. G., Apelqvist, Å. A., Gu, X., Harmon, E. B., Topper, J. N., MacDonald, R. J., & Kim, S. K. (2006). Conditional expression of Smad7 in pancreatic β cells disrupts TGF-β signaling and induces reversible diabetes mellitus. *PLoS biology*, 4(2), e39. PMID: 16435884; PMCID: PMC1351925.

87. Spaeth, J. M., Gupte, M., Perelis, M., Yang, Y. P., Cyphert, H., Guo, S., Liu JH, Guo M, Bass J, Magnuson MA, Wright C, & Stein, R. (2017). Defining a novel role for the Pdx1 transcription factor in islet β-cell maturation and proliferation during weaning. *Diabetes*, *66*(11), 2830-2839. doi: 10.2337/db16-1516. PMID: 28705881; PMCID: PMC5652607.
88. Staffers, D. A., Ferrer, J., Clarke, W. L., & Habener, J. F. (1997). Early-onset type-ll diabetes mellitus (MODY4) linked to IPF1. *Nature genetics*, *17*(2), 138-139. doi: 10.1038/ng1097-138. PMID: 9326926.
89. Statello, L., Guo, C. J., Chen, L. L., & Huarte, M. (2021). Gene regulation by long non-coding RNAs and its biological functions. *Nature reviews Molecular cell biology*, *22*(2), 96-118. doi: 10.1038/s41580-021-00330-4. PMID: 33353982; PMCID: PMC7754182.
90. Stegeman, J. H. (1974). Placental development in the sheep and its relation to fetal development. A qualitative and quantitative anatomic and histologic study. Bijdragen tot de Dierkunde, 44(1), 3-72.
91. Swanson, A. M., & David, A. L. (2015). Animal models of fetal growth restriction: Considerations for translational medicine. *Placenta, 36*(6), 623-630. doi: 10.1016/j.placenta.2015.03.003. PMID: 25819810.
92. Tano K, Mizuno R, Okada T, Rakwal R, Shibato J, Masuo Y, Ijiri K, Akimitsu N. (2010). MALAT-1 enhances cell motility of lung adenocarcinoma cells by influencing the expression of motility-related genes. *FEBS Letters*. *584*(22):4575-80. doi: 10.1016/j.febslet.2010.10.008. PMID: 20937273.
93. Thorn, S. R., Regnault, T. R., Brown, L. D., Rozance, P. J., Keng, J., Roper, M., ... & Friedman, J. E. (2009). Intrauterine growth restriction increases fetal hepatic gluconeogenic capacity and reduces messenger ribonucleic acid translation initiation and nutrient sensing in fetal liver and skeletal muscle. Endocrinology, 150(7), 3021-3030. doi: 10.1210/en.2008-1789. Epub 2009 Apr 2. PMID: 19342452; PMCID: PMC2703533.
94. Thornburg, K., & Louey, S. (2013). Uteroplacental circulation and fetal vascular function and development. *Current vascular pharmacology, 11(*5), 748-757. doi: 10.2174/1570161111311050012. PMID: 24063386; PMCID: PMC7527077.
95. Thureen, P. J., Trembler, K. A., Meschia, G. I. A. C. O. M. O., Makowski, E. L., & Wilkening, R. B. (1992). Placental glucose transport in heat-induced fetal growth retardation. *American Journal of Physiology-Regulatory, Integrative and Comparative Physiology, 263*(3), R578-R585. doi: 10.1152/ajpregu.1992.263.3.R578. PMID: 1415644.
96. Tian H, Wu M, Zhou P, Huang C, Ye C, Wang L. (2018). The long non-coding RNA MALAT1 is increased in renal ischemia-reperfusion injury and inhibits hypoxia-induced inflammation. *Renal Failure*, 40(1):527-533. doi: 10.1080/0886022X.2018.1487863. PMID: 30277425; PMCID: PMC6171433.
97. Tripathi V, Ellis JD, Shen Z, Song DY, Pan Q, Watt AT, Freier SM, Bennett CF, Sharma A, Bubulya PA, Blencowe BJ, Prasanth SG, Prasanth KV. (2010). The nuclear-retained noncoding RNA MALAT1 regulates alternative splicing by modulating SR splicing factor

phosphorylation. *Molecular Cell*. 39(6):925-38. doi: 10.1016/j.molcel.2010.08.011. PMID: 20797886; PMCID: PMC4158944.

98. Van Assche, F. A., Prins, F. D., Aerts, L., & Verjans, M. (1977). The endocrine pancreas in small-for-dates infants. *BJOG: An International Journal of Obstetrics & Gynaecology*, *84*(10), 751-753. doi: 10.1111/j.1471-0528.1977.tb12486.x. PMID: 336076.
99. Yates, D. T., Camacho, L. E., Kelly, A. C., Steyn, L. V., Davis, M. A., Antolic, A. T., ... & Limesand, S. W. (2019). Postnatal β2 adrenergic treatment improves insulin sensitivity in lambs with IUGR but not persistent defects in pancreatic islets or skeletal muscle. The Journal of physiology, 597(24), 5835-5858. doi: 10.1113/JP278726. PMID: 31665811; PMCID: PMC6911010.
100. Yin, D. D., Zhang, E. B., You, L. H., Wang, N., Wang, L. T., Jin, F. Y., ... & Tang, W. (2015). Downregulation of lncRNA TUG1 affects apoptosis and insulin secretion in mouse pancreatic β cells. *Cellular Physiology and Biochemistry*, *35*(5), 1892-1904. doi: 10.1159/000373999. PMID: 25871529.
101. Watts R, Johnsen VL, Shearer J, Hittel DS. Myostatin-induced inhibition of the long noncoding RNA Malat1 is associated with decreased myogenesis. (2013). *American Journal of Physiology-Cell Physiology*. *304*(10):C995-1001. doi: 10.1152/ajpcell.00392.2012. PMID: 23485710.
102. Wu, W., Hu, Q., Nie, E., Yu, T., Wu, Y., Zhi, T., ... & You, Y. (2017). Hypoxia induces H19 expression through direct and indirect Hif-1α activity, promoting oncogenic effects in glioblastoma. *Scientific reports*, 7(1), 45029. doi: 10.1038/srep45029. PMID: 28327666; PMCID: PMC5361208.
103. You, L., Wang, N., Yin, D., Wang, L., Jin, F., Zhu, Y., ... & De, W. (2016). Downregulation of long noncoding RNA Meg3 affects insulin synthesis and secretion in mouse pancreatic beta cells. *Journal of cellular physiology*, *231*(4), 852-862. doi: 10.1002/jcp.25175. PMID: 26313443.
104. Zhang, X., Hamblin, M. H., & Yin, K. J. (2017). The long noncoding RNA Malat1: Its physiological and pathophysiological functions. *RNA biology*, *14*(12), 1705-1714. doi: 10.1080/15476286.2017.1358347. PMID: 28837398; PMCID: PMC5731810.
105. Zhang, X., Wang, W., Zhu, W., Dong, J., Cheng, Y., Yin, Z., & Shen, F. (2019). Mechanisms and functions of long non-coding RNAs at multiple regulatory levels. *International journal of molecular sciences*, *20*(22), 5573. doi: 10.3390/ijms20225573. PMID: 31717266; PMCID: PMC6888083.
106. Zhao G, Su Z, Song D, Mao Y, Mao X. (2016). The long noncoding RNA MALAT1 regulates the lipopolysaccharide-induced inflammatory response through its interaction with NF-κB. *FEBS Letters*, 590(17):2884-95. doi: 10.1002/1873-3468.12315. PMID: 27434861.